PREPARATION AND CHARACTERIZATION OF A CERAMIC ULTRAFILTRATION MEMBRANE BY SOL GEL METHOD

by

IVAN SAHA

MATERIALS SCIENCE PROGRAMME

INDIAN INSTITUTE OF TECHNOLOGY KANPUR

JULY, 1994

To my Parents

CERTIFICATE

This is to certify that this work on PREPARATION AND CHARACTERIZATION OF A CERAMIC ULTRAFILTRATION MEMBRANE BY SOL GEL METHOD by Ivan Saha has been carried out under our supervision and that this has not been submitted elsewhere for any degree

(S Bhatia) 28/7/94
Professor
Department of Chemical Engineering
Indian Institute of Technology
Kanpur 208016

(D C Agrawal) 28/7/94
Professor
Materials Science Programme
Indian Institute of Technology
Kanpur 208016

July 1994

ACKNOWLEDGEMENTS

In the very beginning I would like to express my deep sense of gratitude to Dr D C Agrawal and Dr S Bhatia for their constant guidance and encouragement during the course of this work It was Dr D C Agrawal who introduced me to this field and helped develop my interest in it for which I am indebted to him The helpful discussions with Dr P K Bhattacharya and his kind consent to work in his laboratory is gratefully acknowledged

Thanks are also due to Sirsendu and Subir for their indespensible help during the conduct of experiments

Help rendered by Santanu Ajai Murali Subhasish Atanu and Umamahesh will be remembered forever All of them and others like Manab Debangshu Sanjeev Viji Seema and Sangita made my stay here a memorable one

The bonhomie of my Hall-4 friends like Ranganda Mama Biswarupda and Sankarda add to the nostalgia that is associated with this place

My parents and all near and dear ones have all been a silent source of motivation for me

Ivan Saha

CONTENTS

LIST OF FIGURES

LIST OF TABLES

1INTRODUCTION

1 1 HISTORICAL BACKGROUND AND OVERVIEW

1 1 1 Membrane development over the years

Membranes have been known from the time osmosis was discovered In 1748 Abbe Nollet observed the phenomenon of osmosis which is the transport of water or solvent through a semi-permeable membrane [defined as a membrane which is permeable to solvent and impermeable to solutes] from a dilute solution to a more concentrated solution Matteucci and Cima (1845) and later Schmidt (1856) observed that these membranes tend to be anisotropic in nature i e their behaviour was different depending on which side of the membrane faced the feed solution [1]

The first synthetic membrane made of nitrocellulose was made by Fick in 1865 In 1877 Pfeffer reported the manufacture of membranes by precipitating copper ferrocyanide in the pores of porcelain Later the interest shifted to membranes made of collodion a term used for cellulosic polymers Graham in 1854 was probably the first to use a membrane for separations He used it as a dialyser to separate a solution into its components [2] Around the year 1907 Bechhold developed methods for controlling the pore size of these collodion membranes He suggested the use of air pressure for improved permeability and developed methods for measuring pore diameters using air pressure and surface tension measurements He is the first researcher to come up with the term ultrafiltration The theories of thermodynamics of solutions developed by Van t Hoff and later Gibb s led to the thermodynamic understanding of the membrane processes From 1927 [2] membrane filters became commercially available They were manufactured using the Zsigmondy Process by the Sartorius Company in Germany

Till 1945 membrane filters were primarily used for removal of micro-organisms and particles from liquid and gaseous streams for diffusion

studies and sizing of macromolecules German scientists in 1951 developed methods for culturing bacteria cells on membranes In 1957 the United States Public Health Service officially adopted the membrane filtration procedure for drinking water analysis

In early 1950 Samuel Yuster of the University of California LA had predicted based on Gibb s adsorption isotherm it would be possible to produce fresh water from brine S Sourirajan working in the same University reported some success with this concept Using a hand operate pump he managed to produce a few millilitres of fresh water over a few days [2] However as seen in Table 1 1 first row the flux was very low although 94/ salt rejection was obtained

Table 1 1 Development of homogeneous and asymmetric membranes [2]

Investigator	Morphology	ΔP_T (Psig)	Flux (LMH)*	% NaCl rejection
Yuster et al (1958)	Homogeneous	800	0 05	94
Loeb and Sourirajan (1963)	Asymmetric (Commercial)	1103	3 0	92
Loeb and Sourirajan (1963)	Asymmetric (L-S)**	1070	14 5	99

* LMH - Litres per m^2 per hr

** L-S - Loeb - Sourirajan membrane

From 1958 to 1960 Sourirajan and Loeb attempted to modify commercial cellulose acetate membranes by heating them under water in the hope that this would expand the pores and that the pores would remain open as the

membrane cooled thus increasing the flux But the opposite happened Heating contracted the pores This increased the salt rejection and interestingly increased the flux ! This apparent anomaly can be explained by the fact that the heating process created a phenomenon called anisotropy or asymmetry in the ultrastructure of the membrane an observation made about 100 years ago on natural membranes The anisotropy is due to a thin skin on one surface of the membrane usually 0 1 - 0 2 μm thick while the main body is sponge like with porous voids Since the major resistance to flux is the membrane thickness lowering the effective thickness led to greatly improved flux The smaller pore size led to higher salt rejection as shown in 2nd and 3rd row of Table 1 1

This single development of asymmetric membrane is what converted a laboratory curiosity into a practical and viable unit operation for the chemical biological pharmaceutical and food processing industry

The history of ceramic inorganic membranes date back to the 1940 s when Vycor-type glass membranes had been synthesized They usually had a very inconsistent pore size distribution [3] Dynamic inorganic membranes formed by filtering colloidal solutions through porous filters [4] have the disadvantage that flux decline is so large after a few weeks of operation that replacement is inevitable A third type of inorganic membranes have been produced by Union Carbide They are referred to as Ucarsep [5] and are formed by placing ultra stabilized zirconia on a silica support While these membranes have a wide range of pH stability they have fairly high molecular weight cut off values because of their large pore size

The sol-gel process for producing uniformly size powders introduced in early 1940 s has been used for the last 20 years to prepare UO_2 pellets for nuclear reactors Yoldas [6 7,8] revolutionized the field by producing porous transparent alumina from alkoxide precursors and found that

the peptizing acid added influence to the sol-gel transformation and the ability of the gel to retain its integrity Kaiser and Schimidt [8] used alkoxysilanes to deposit porous silica membranes (5 - 10 μm thick) on porous supports These silica membranes had a mean pore diameter of 2 5 nm and a specific surface area of 200-300 m^2/gm

It was after the pioneering work of Leenaars and Burggraaf [10 11 12 13] that the idea of commercial ceramic membranes became feasible Leenaars et al used the Yoldas method to prepare boehmite sol which was slip cast on to α-Al_2O_3 supports By controlling sol pH alumina concentration and calcination temperature they were able to prepare membranes with ultrafine pores and narrow pore size distribution These membranes had cut off values 10 times lower than those of Ucarsep membranes and they also offered greater stability than either Vycor or dynamic membranes

1 1 2 Definition and classification of membranes

The primary role of a membrane is to act as a selective barrier It should permit passage of certain components and retain certain other components Hwang and Kammermeyer have defined a membrane in its broadest sense as a region of discontinuity interposed between two phases Lakshmionarayanaiah (1984) refers to a membrane as a phase that acts as a barrier to prevent mass movement but allows restricted and/or regulated passage of one or more species through it [2] According to Ho and Sirkar [14] a membrane is an interphase between two bulk phases It is either a homogeneous or a heterogeneous collection of phases

A MEMBRANE PROCESS ¦

The membrane phase interposed between two bulk phases control the exchange of mass between the two bulk phases in a membrane process In a membrane process the two bulk phases are mixtures One of the species in the mixture is allowed to be exchanged in preference to others One

bulk phase is enriched in one species while the other is depleted of it A membrane process thus allows selective and controlled transfer of one species from one bulk phase to another bulk phase separated by a membrane

The movement of any species across the membrane is caused by one or more driving forces These may be due to a gradient in chemical or electrical potential The transmembrane flux of any species per unit driving force is proportional to the permeability of the species If the driving force is defined by a partial pressure difference (ΔP_1) or concentration difference (ΔC_1) across the membrane for species 1 then

$$\text{Transmembrane flux of species 1} = \frac{\text{Permeability of species 1}}{\text{membrane thickness}} \times (\Delta P_i \text{ or } \Delta C_i)$$

The ratio permeability of species 1/membrane thickness is called the permeance

The membrane selectivity between any two species can be defined by a separation factor α_{ij} which for two species 1 and J is

$$\alpha_{ij} = \frac{C_i' / C_j'}{C_i'' / C_j''}$$

where the prime and double prime superscripts denote the upstream bulk phase (feed) and downstream bulk phase (permeate) respectively

The separation factor is equal to the ratio of the two liquid permeabilities under conditions in which the downstream pressure or concentration is negligible in comparison to the upstream pressure or concentration

Membranes can be classified on the basis of their

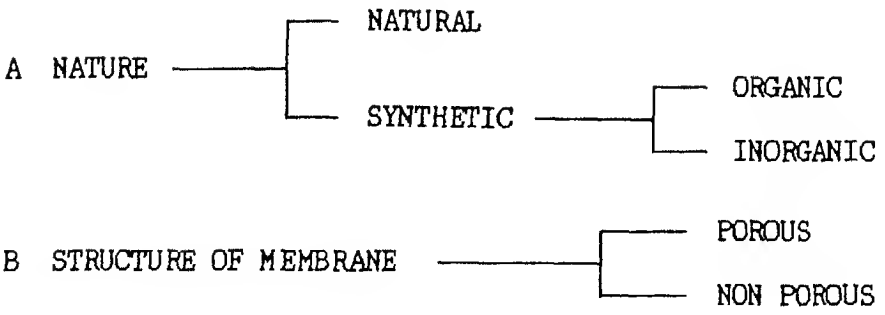

C APPLICATION OF MEMBRANE

1 GASEOUS PHASE SEPARATION

2 GAS - LIQUID PHASE SEPARATION

3 LIQUID - LIQUID PHASE SEPARATION

4 SOLID - LIQUID PHASE SEPARATION

D MECHANISM OF MEMBRANE SEPARATION

1 OSMOTIC

2 DIALYSIS

3 ULTRAFILTRATION

4 REVERSE OSMOSIS

5 ELECTRO DIALYSIS

6 MICROFILTRATION

Membranes can also physically or chemically modify the permeating species (as with ion-exchange or bio-functional membrane) conduct electric current prevent permeation (e g in packaging or coating applications) or regulate the rate of permeation (as in controlled release technology) Ionogenic groups and pores in membranes confer properties as permselectivity and semi-permeability

Fig 1 1 [2] shows a classification of the various

separation processes based on particle or molecular size as the primary factor affecting the separation process. The five major membrane separation processes viz. reverse osmosis, ultrafiltration, microfiltration, dialysis and electrodialysis cover a wide range of particle size matched in versatility only by centrifugal processes. However an absolute requirement for centrifugal processes is the existence of suitable density difference between the two phases that are to be separated , in addition the two phases must be immiscible. Membrane separation processes have no such requirement and the real value of ultrafiltration and reverse osmosis is that they permit separation of dissolved molecules down to the ionic range, provided the appropriate membrane is used.

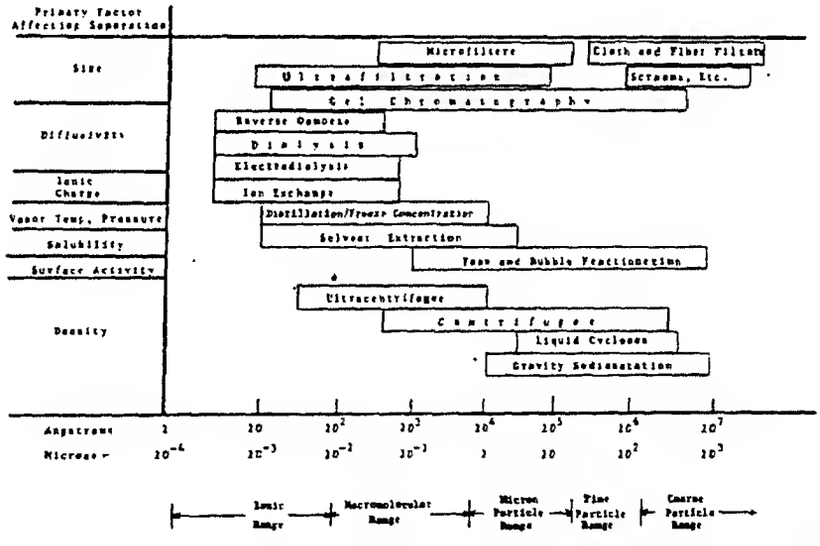

Fig.1.1. Useful range of separation processes showing the range of particle or molecular size covered by each process and the primary factors governing each separation process [2].

Among membrane processes itself the distinction is quite arbitrary and one usually merges with the other However a set of definition is attempted at this stage of the various separation processes

A OSMOSIS is the transport of solvent through a semipermeable membrane from the dilute solution side to the concentrated solution side of the membrane It is driven by the chemical potential difference of the solvent across the membrane

B REVERSE OSMOSIS is the pumping of the feed solution under pressure over the surface of a suitably supported membrane RO results in retention of macromolecules in the feed solution (retentate) and depletion in the permeate solution This effectively results in concentrating the original feed A typical RO membrane has pore sizes < 1 nm and has a molecular weight cut off (MWCO) of < 100 Daltons

C ULTRAFILTRATION is also primarily a size-exclusion-based pressure-driven membrane separation process UF membranes have typical pore sizes in the range of 1 - 100 nm and are capable of retaining species in the molecular range of 300 - 500 000 Daltons The MWCO of a UF membrane is defined as the smallest molecular weight species for which the membrane has over 90% rejection

D MICROFILTRATION when pressure driven flow through a membrane or other filter medium is used to separate micron-sized particles from fluids the process is called microfiltration Although the exact size range is open to debate it generally refers to the filtering of a suspension containing colloidal or fine particles with linear dimensions in the range of 0 02 to 10 microns

E DIALYSIS is a rate governed membrane process in which a microsolute is driven across a semipermeable membrane by means of a concentration gradient The microsolute diffuses through the membrane at a greater rate than macrosolutes also present in the feed solution If the receiving solution

(defined as dialysate) is not continuously renewed the solute concentrations on both sides of the membrane will tend to equalize negating the driving force for the separation This is an essential difference between an equilibrium-based process and a rate-governed membrane process

F ELECTRODIALYSIS is an electrochemical separation process in which electrically charged membranes and an electrical potential difference are used to separate ionic species from an aqueous solution and other uncharged components

Table 1 2 shows the characteristics of the ideal membrane processes [2]

Process	Driving Force	Permeate	Retentate*
Osmosis	Chemical Potential	Water	Solutes
Dialysis	Concentration Difference	Water + Small Molecules	Large Molecules
Ultrafiltration	Pressure	Water + Small Molecules	Large Molecules
Reverse Osmosis	Pressure	Water	Solutes
Electrodialysis	E M F	Water + Ionic Solutes	Nonionic Solutes
Microfiltration	Pressure	Water + Dissolved Solutes	Large Suspended Particles

Also includes water

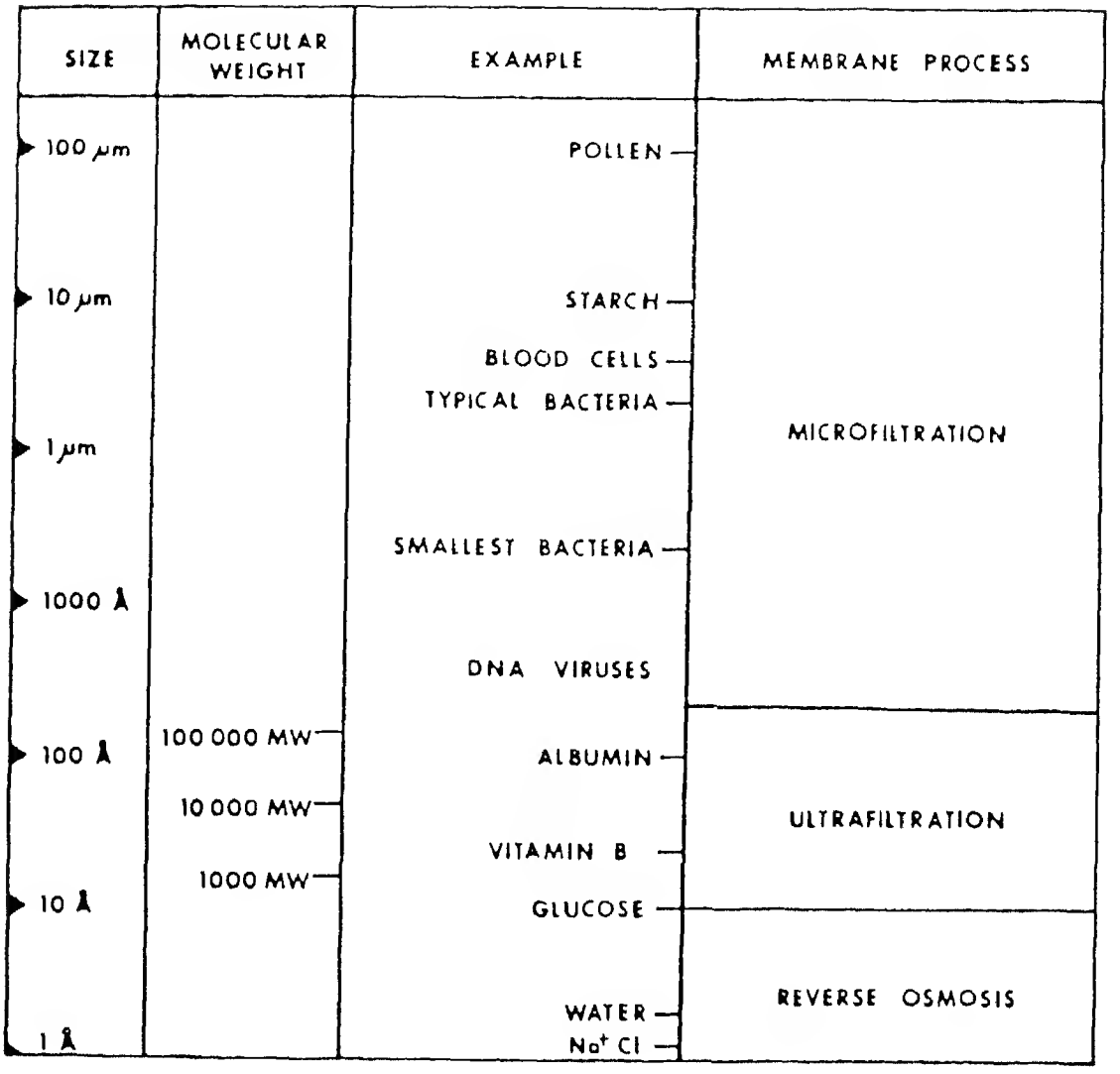

Fig 1 2 Examples of components separated by MF UF and RO membranes [2]

UF and RO membrane separation processes enjoy a number of advantages over other comparable processes

1 UF and RO constitute a continuous molecular separation process that do not involve a phase change or interphase mass transfer making it particularly exciting for fields like food processing pharmaceutical and biological

2 Because ultrafiltration deals with the separation of fairly large molecules e g proteins starch clays paints etc the osmotic pressures involved in ultrafiltration processes are fairly low Thus UF offers the advantage of needing fairly low pressures for operations which will reduce equipment costs

3 UF and RO processes can be operated at ambient temperatures without complicated heat transfer or heat generating systems as used in the dewatering process

The limitations of UF and RO processes are that

1 None can take solutes to dryness In RO process the upper limit is the osmotic pressure of the concentrated solutes In UF the rather low mass transfer rates of large macromolecules is the limiting factor

2 Other problems that plague membrane application are fouling of membranes poor cleanability and restricted operating conditions These have been partially overcome by superior membrane materials and better designed membrane modules

1 1 3 Why ceramic membranes

Polymeric membranes have been commercially available for many years They have been incorporated in large scale applications in a host of industrial processes However these membranes suffer from inherent polymeric properties Dry atmospheres non aqueous organic solvents and high temperature (> 250°C) might cause a collapse of the membrane structure and

the membrane might lose its permeability High or low pH can result in hydrolysis of membrane material which is also prone to enzyme or microbial attack These problems can be alleviated and the horizon of membrane application can be further expanded by the use of inorganic membranes

Two categories of inorganic membranes can be distinguished non porous and porous Non porous metallic or oxide membranes exhibit high selectivities but lower permeabilities due to the activated solution - diffusion transport mechanism involved [15] The metallic membranes are not so stable to repeated adsorption/desorption cycles use under steam-containing conditions or at elevated temperatures Glass membranes are found to be of irregular pore size distributions which is difficult to control The remaining category is that of ceramic membrane Membrane made of γ - Al_2O_3 ZrO_2 TiO_2 UO_2 and their composites have been found to be candidate materials for a myriad of new technologies Indeed with the advent of ceramic membranes in the market the potential use of membrane processes in varied fields as biotechnology to nuclear waste treatment has multiplied manifold Ceramic membranes offer a number of distinct advantages over its glass metallic or polymeric counterparts

1 Chemical stability Ceramic membranes can withstand corrosive inorganic/organic solvents and pH extremes

2 High temperature application Ceramic membranes are stable at very high temperature without loss of membrane ultrastructure, allowing sterilization of process equipment for food and pharmaceutical applications and also for high temperature membrane reactors

3 Stability to microbial degradation These membranes are immune to biological attack

4 Mechanical stability Unlike polymeric membranes which compact under high pressures ceramic membranes posses high mechanical strength

5 Cleaning conditions Items 1 2 and 3 indicate more harsher and effective cleaning treatments can be used with ceramic membranes

The only reason for their albeit slow penetration of the membrane market is their relatively higher cost of production If this can be offset by their longer life then this group of membranes which presently account for 5-10% of the market share of their polymeric rivals can surely dominate the membrane market

1 2 APPLICATION AREAS AND ECONOMIC PROSPECTS OF CERAMIC MEMBRANES

1 2 1 Application of ceramic membrane systems

The application areas of ceramic membranes are tabulated in Table 1 3 along with the desired properties that are asked for in a particular application

Membrane processes are used widely in the following industries

A THE DAIRY INDUSTRY

Ultrafiltration is an accepted processing operation in the dairy industry The two largest application are in the preconcentration of milk for cheese manufacture and the fractionation of cheese whey to give whey proteins

B BIOTECHNOLOGY

It is the glamorous description of a wide range of biological processes that can be used for the production of a variety of products from foods flavours organic chemicals and pharmaceutical to fuels and agricultural chemicals The many applications are in the areas of

1 Separation and harvesting of enzymes and microorganisms
2 Continuous high performance bio-reactors for enzymatic and microbial conversion process
3 Tissue culture reactor systems
4 Production of pure, high quality water

Table 1 3 Application and application possibilities of ceramic membranes [16]

Type of application	Industry	Remarks
Microfiltration Ultrafiltration and Reverse - Osmosis	Milk beverage	good resistance to cleaning in alkaline media
	biotechnology & pharmaceutical	steam sterilization
	textile engineering and paper	high temperature resistance
	oil	high temperature and solvent resistance
Gas separation	petrochemical industry	high temperatures high selectivity and permeability for H_2 CO_2 O_2
Membrane Reactors	petrochemical	high temperature dehydrogenation partial oxidation catalytically active
	environmental	removal of NO_2 and SO_2 high temperature catalytically active

C TEXTILE INDUSTRY

Ultrafiltration and reverse osmosis are mainly used for the recovery of expensive synthetic sizing agents like carboxymethyl cellulose and polyvinyl alcohol from the waste stream Also recovery of indigo dye out of textile waste water is done by ultrafiltration membrane systems

D PULP AND PAPER INDUSTRY

The paper industry produces about 100 000 litres of highly polluted bleach liquor per ton of pulp Ultrafiltration is used to concentrate and recycle some of the effluents prior to discharge Membranes with MWCO values of 3000 - 5000 are most promising in these applications

E MEMBRANE REACTORS

In recent years the application of ceramic membrane reactors operated at high temperatures have attracted much attention [15 16]

In a high temperature reactor the in corporation of membranes can serve three different purposes

1 Enhancement of the conversion of a chemical reaction i e by shifting the equilibrium situation by selective removal of one of the reaction products

2 To influence the path of the chemical reaction i e to increase the reaction selectivity

3 To obtain special effects i e to avoid or decrease catalyst deactivation

Two membrane categories can be distinguished on the basis of its function in the reactor [16]

A Passive

B Catalytically active membrane

The case of passive membrane is shown in Fig 1 3 The membrane is used here exclusively for separation function The case shown is an equilibrium limited dehydrogenation reaction which is considerably shifted to higher conversion by selectively removing H_2 from the equilibrium The catalyst does not form an integral part of the membrane but is loosely kept on the membrane

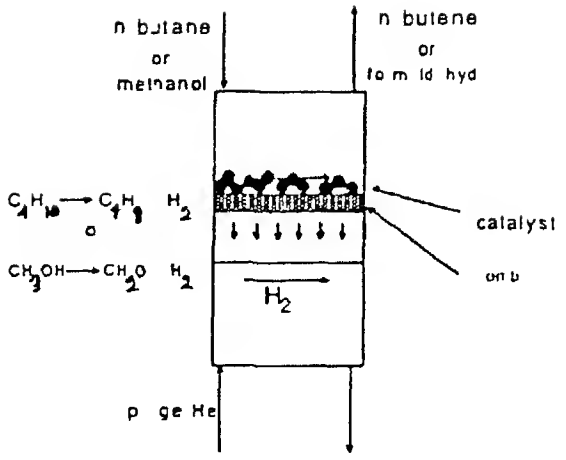

Dehydrogenation of n butane or methanol

FIGURE 13 Schematic diagram of the passive membrane reactor operation

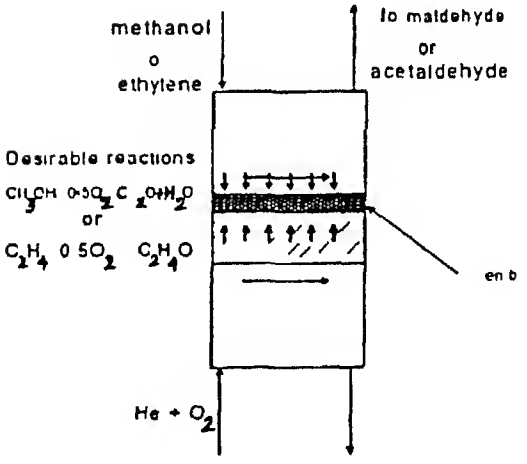

Partial oxidation of methanol or ethylene

FIGURE 14 Schematic diagram of a catalytically active membrane reactor

In Fig 1 4 the catalytically active membrane reactor is shown The catalytic activity is bound to the membrane being either an inherent property of the material or a property added to the membrane by modification with catalytically active phase within the pores (or as a thin layer on top of it)

A recent paper [17] by Zaspalis et al gives examples of this concept Zaspalis used a catalytically active membrane [Fig 1 4] containing a top layer of γ - Al_2O_3 (pore diameter 4 nm) modified with a V_2O_5 catalyst for selective oxidation of ethylene to acetaldehyde With the supply of oxygen from the support side the undesirable reaction of total oxidation to CO_2 could be avoided At 300 C the selectivity of acetaldehyde increased from 20% to 70% while the total conversion decreased from 70% to 25% The case of butane dehydrogenation to butene has also been discussed by Zaspalis [17] Here the passive membrane is γ - Al_2O_3 [with 4 nm pore diameter] The catalyst was Pt/SiO_2 At 500 C the selectivity and conversion increased from 40% to 60% and 9% to 15% respectively compared to packed bed reactor

Sun [15] studied the dehydrogenation of cyclohexane He used a γ - Al_2O_3 membrane and Pt/SiO_2 pellets as the catalyst He reported conversion of 40% compared to equilibrium conversion 26%

1 2 2 Economic evaluation of ceramic membrane technology

Membranes and membrane process have become industrial products of considerable commercial and technological importance Membranes are used nowadays to produce potable water from sea water, to treat industrial effluents, to fractionate to concentrate and purify molecular solutions in chemical and pharmaceutical industries In 1988 the world wide sales of synthetic membranes was projected to be 1 2 x 10^9 US$ with an annual increase of 12 to 14%

The entire range of membrane processes and industrial applications in order of their state of technical development which in certain application can be regarded as status - of - the - art is shown in Fig 1 5 In other applications the same processes are only used on a pilot plant scale and in others they are just tested in the laboratory

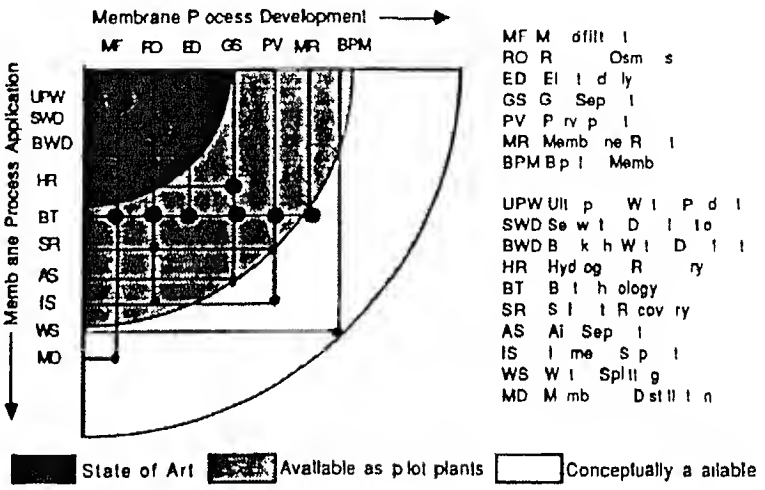

Fig 1 5 Schematic diagram showing membrane separation processes and their application as a function of status of development [18]

According to Burggraaf [16] the market of inorganic membranes is only 5 - 10% of that of the polymeric membranes Crull analyzed the market trends of inorganic membrane for micro and ultrafiltration application and predicted a spectacular growth between the year 1995 and 2000 Fain [16] predicts an even more fantastic growth only if the costs are reduced to 1/3 of present and separation factors are increased

The realized and projected sales of inorganic membranes as given by Crull is shown in Table 1 4

Table 1 4 Realized and projected sales of inorganic membranes [16]

Material	1986	1989	1994	1999	growth %
		in million US dollars			
Ceramics	6	18	75	345	34
Carbon	Ø	3	8	5Ø	32
Metals	5	8	13	25	12
Glass	Ø	Ø	1	3	>1ØØ
Other	1	2	4	9	16
Total	12	31	1Ø2	432	3Ø

The main conclusion is that inorganic membrane systems especially ceramic membranes have tremendous potential for high technology applications But their commercialization has been deterred by their high costs and low separation factors Once these handicaps are overcome these new class of membranes can be pushed to the very frontiers of membrane technology

1 3 STRUCTURAL ASPECTS AND MAIN PREPARATION METHODS

1 3 1 Structural aspects

Burggraaf and co - workers [15] classified inorganic membranes into two groups i) dense and ii) porous Both can be subdivided into i) supported and ii) unsupported membranes

The essential structural features of the porous membranes are shown in Fig 1 6 As seen from the figure there can be various kinds of pore systems straight pores running from one side of the membrane to the other having constant pore diameter or with conical pores as shown in Fig 1 6 (a) and (b) respectively These types of systems can be correlated to track etch and anodic oxidation processes respectively The system shown in Fig 1 6 (c) shows a percolation system of pores with interconnected porosity

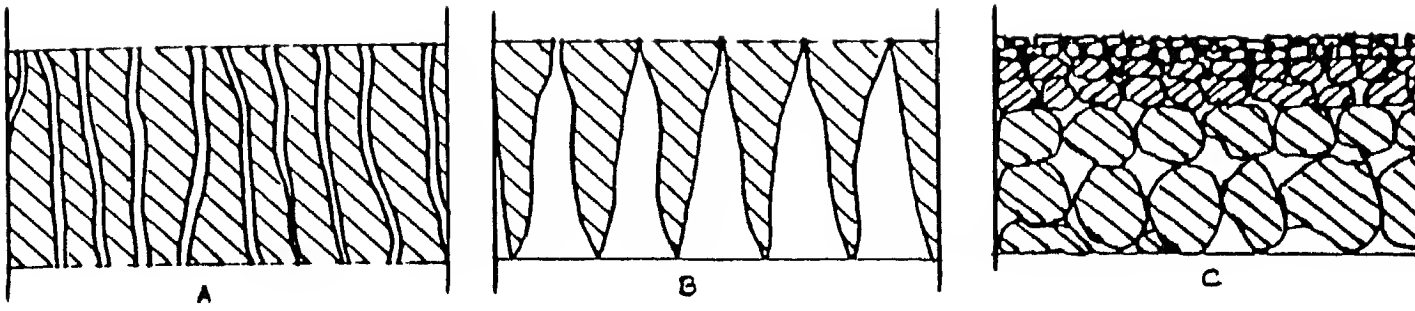

FIGURE 16
Schematic representation of main type of pore structures in membranes A and B homogeneous unsupported straight pore systems C supported interconnected pore system

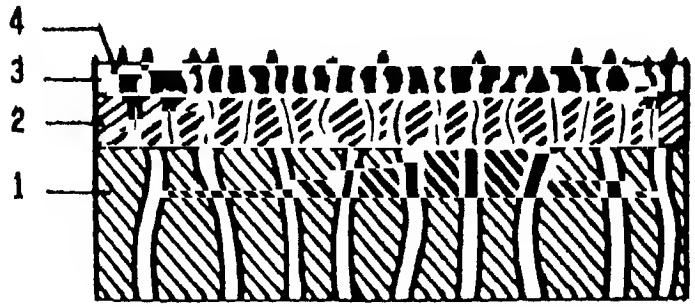

FIGURE 17
Schematic representation of an asymmetric composite membrane 1) porous support with d_p=1-15 µm d_l=1 2 mm 2) intermediate layer with d_p 0 1 1 5 µm d_l 20-100 µm 3) separation (top)layer with d_p 3 100 nm d_l=1-10 µm 4) modification of separation layer d_p-pore diameter d_l- layer thickness

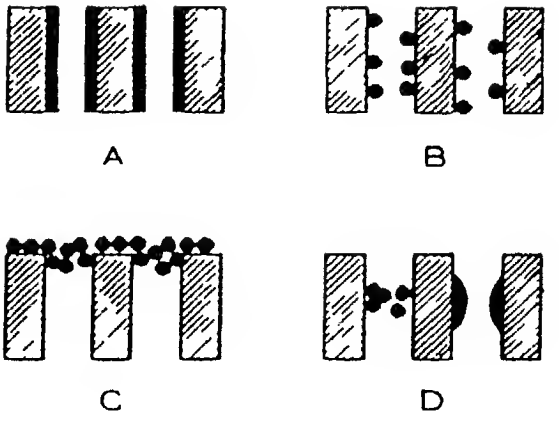

FIGURE 18

Schematic representation of the microstructure of a modified (catalytic) membrane toplayer A) mono or multilayer deposit B) micro(nano) particles within pore partial plugging C) plugs in the pore entrance film on top of the membrane D) plugs or constrictions on certain site within the pore

and progressively finer pore size This is the typical configuration of asymmetric ceramic membranes

To obtain large flux values the membrane separation layer should be very thin Therefore thin films are supported by thick microporous support materials Such a combination yields an asymmetric system which combines mechanical stability with low flow resistance Such a composite system consists of 2 to 3 layers as shown in Fig 1 7 This type of ceramic membrane is used most frequently

The thin top layer can have 30 - 50% porosity and pore diameters as small as 3 nm They are made of γ - Al_2O_3 TiO_2 ZrO_2 and their mixtures on α - Al_2O_3 supports

The top layer can be modified by a variety of methods principally resulting in 4 types of nanostructures as shown in Fig 1 8

In this way the pore diameters can be decreased and the chemical nature of the internal surface can be modified [19 20]

1 3 2 Preparation methods

Porous inorganic membranes can be prepared by various ways depending on materials membrane and support structures pore size porosity and membrane thickness Summarizing some of these methods [21]

1 PHASE SEPARATION AND LEACHING

Usually glass membranes are prepared in this way First the glass matrix is separated into two phases by thermal treatment One of the phases (Na_2O -B_2O_3 rich phase) is then preferentially water or acid leached thereby creating a microporous SiO_2 - rich phase that can act as a membrane

2 ANODIC OXIDATION

One side of an aluminium foil is anodically oxidised in an acid electrolyte The unaffected side is subsequently leached away with a strong acid These membranes generally consist of two regions a bulk porous

layer and a thin fine - pore selective membrane layer adjacent to the metal The pore diameter depends strongly on the electrolyte used e g H_2SO_4 H_3PO_4 oxalic acid etc Usually a hydrothermal treatment at 35 - 80 C is subsequently needed to improve membrane stability

3 PYROLYSIS

Certain porous inorganic membranes can be derived by pyrolysis of organic polymers SiO_2 and carbon molecular sieves can be obtained by pyrolysing silicone rubber and certain thermoset polymers, respectively

4 TRACK ETCH METHOD

When a radioactive source is used to pass particles through a material the track left behind is highly sensitive to an etchant as conc HF After etching the resulting material is a membrane with straight pores of uniform size and shape

5 SOL - GEL ROUTE

This is by far the most important process of manufacture of ultrathin membranes on a porous support The fine structure of the membranes can be tailored to a great extent by the processing parameters thus making the membranes suitable for a whole range of application Commercially available Al_2O_3 ZrO_2 and TiO_2 membranes are made by this method A metal alkoxide is hydrolysed to form a stable sol This is used to coat a porous support (usually α - Al_2O_3) by a slip - casting technique The composite membrane is then calcined at a temperature that causes crystallisation of the top layer and the formation of nanometer sized pores The great volume of literature published on this method of membrane preparation is an indication of its importance in ceramic membrane synthesis

1 3 3 Membrane preparation by the sol gel method

Membranes of silica titania zirconia and alumina are usually prepared by the sol - gel method The process mainly involves hydrolysis of metal salts or alkoxides followed by polycondensation of the hydroxylated species In gelation the moles or particles connect to form a three dimensional network Brinker and Scherer [30] have discussed the solution chemistry of transition metals silicate and aluminates It is imperative to understand the chemistry itself in order to exploit the process for making membranes

A THE SOL GEL PROCESS

Transition metal alkoxides (Ti Zr) are used widely as precursors to glasses and ceramics In the absence of catalysts the hydrolysis and condensation occur by the following reactions

a Hydrolysis

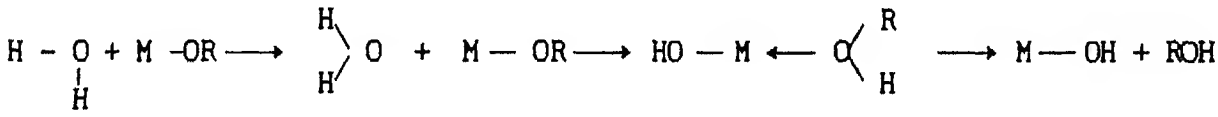

b Alcoxolation

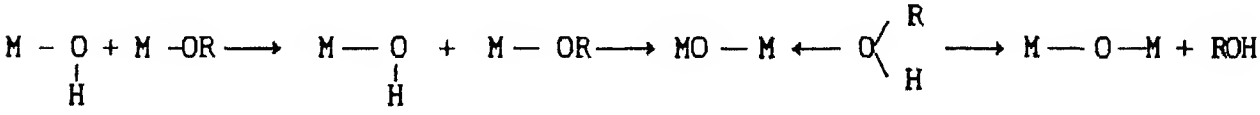

c Oxolation

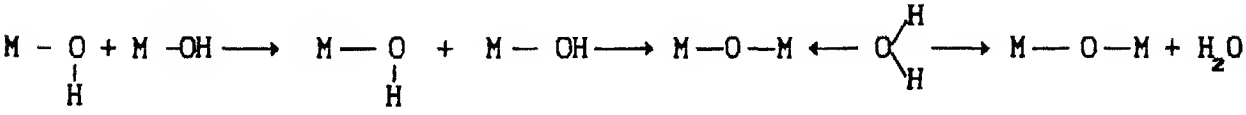

d Olation

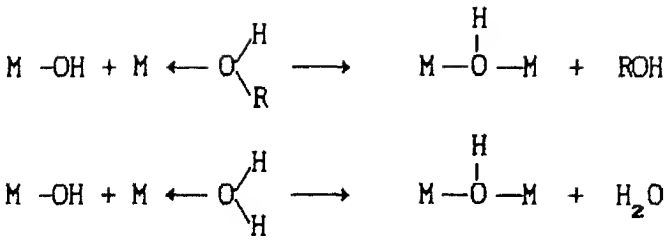

Acids or base can influence both the hydrolysis and condensation rates and the structure of the condensed product Acid catalysed condensation results in more extended less highly branched polymers The opposite is true when bases act as catalysts The structure of the condensed product depends on the relative rates of the four reactions When water alkoxide ratio (r) is greater than 2 precipitation of hydroxide occurs For low r values and carefully controlled hydrolysis oxo - alkoxide products are formed Addition of chemical modifiers like chelating agents lead to more complex structures

In the case of silicon alkoxides hydrolysis and condensation is defined by three reactions

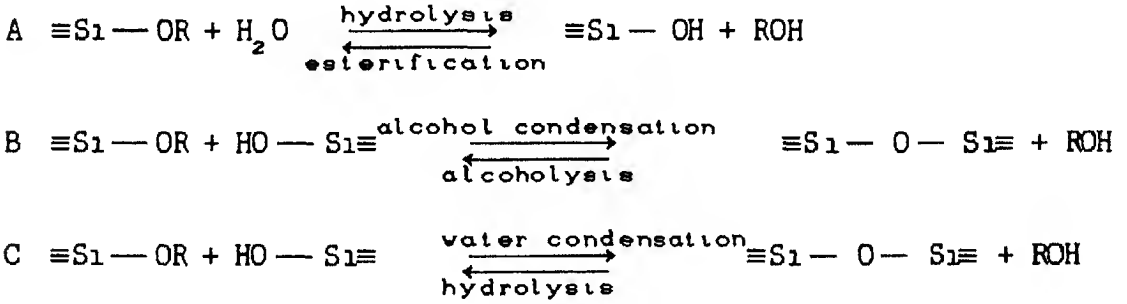

The rates of these reactions are governed by the pH temperature steric and inductive effects of various side groups and the type of solvent used

The solution chemistry of aluminium alkoxides is similar to that of transition metal alkoxides The discovery of Yoldas [6,7,8] that

the hydrolysis and condensation of aluminium alkoxides can result in monolithic alumina gels is infact responsible for the explosion in sol - gel research that continues to this day

The Yoldas process is outlined in Fig 1 9

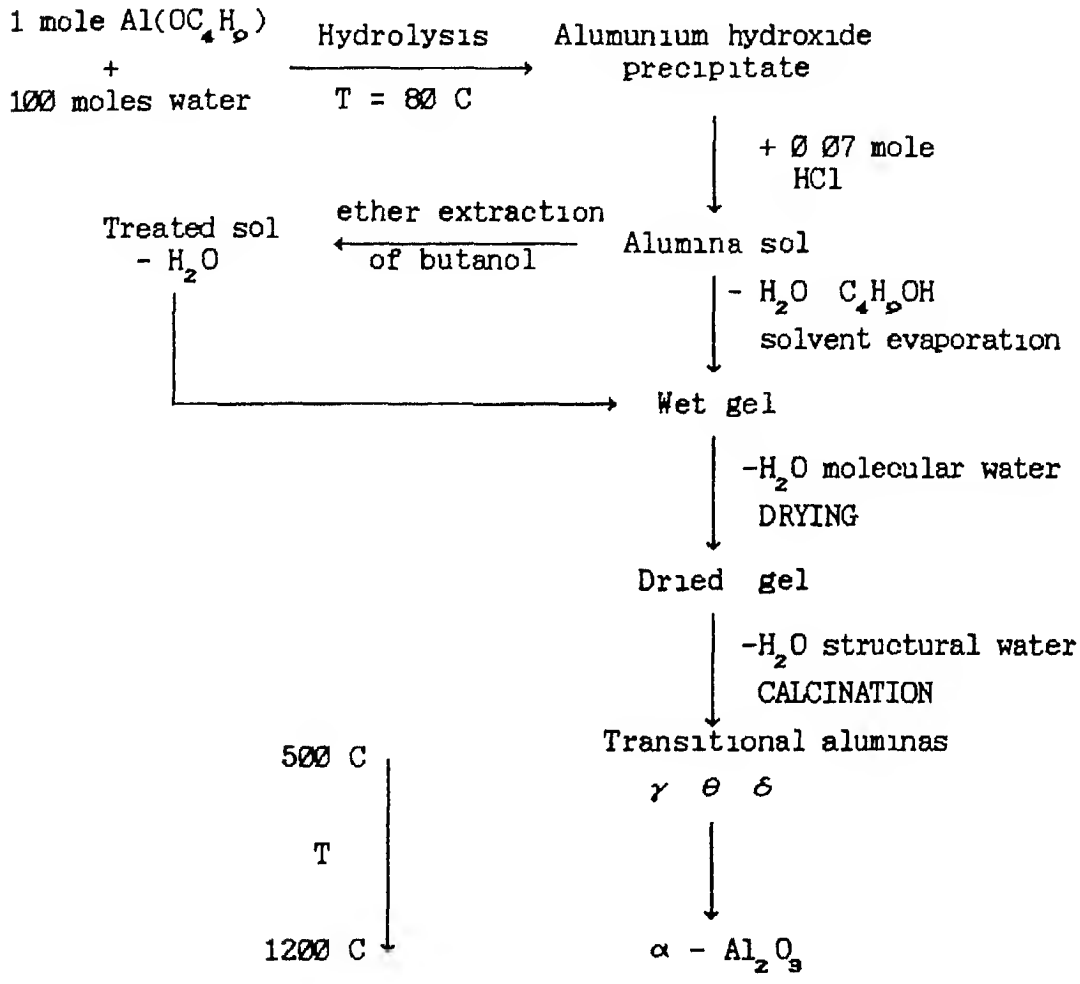

Fig 1 9 The Yoldas Process [30]

Yoldas prepared sols with different acid concentrations and types He reported a minimum gelling volume at acid Al molar ratio of 0 07 A minimum acid concentration (0 03) moles per mole of alkoxide) is needed for complete peptization If more than 0 1 mole of acid is used, gel does not form monolithic alumina There appears to be two requirements for the type of acid

1 The anions must be non complexing (or very weakly complexing) with aluminium ions at low concentrations Hence sulphuric and hydrofluoric acids do not peptize

2 The amount of acid in relation to aluminium must not be large enough to prevent the formation of a continuous aluminium bonding through oxygen (oxalated) or through hydroxides (olated) This rules out organic acids in this process

Temperature is very important in producing a clear sol Sols held at 80 C for a few hours peptizes completely due to the removal of residual (OR) groups in the hydroxide

Particle size and shape is also affected by the amount of acid used as shown in Table 1 5 Higher acid concentrations produced more fibrillar boehmite crystals

Table 1 5 Effect of acid concentration on particle size of alumina sols [8]

Acid/alkoxide ratio (mole mole)	Size
0 02	50 - 350 Å round
0 035	50 - 350 Å round
0 07	100 - 200 Å width 400 - 500 Å length
0 14	100 - 200 Å width 100 - 1000 Å length
0 21	100 - 200 Å width 100 - 1000 Å length

Structural evolution during the Yoldas process has been documented by various groups using techniques as MAS - NMR Raman spectroscopy and IR studies Assih et al [3] reported octahedral aluminium species (0 - ppm) as well as a broad tetrahedral resonance at 60 - 70 ppm using ^{27} Al NMR The corresponding Raman spectra showed a peak at 360 cm^{-1} which correlated to the 0 - ppm ^{27} Al NMR resonance

B The evolution of the transition aluminas

Alumina prepared by Yoldas methods remains the most thoroughly studied crystalline gel system Xerogels which are composed of boehmite (γ - AlOOH) or pseudo - boehmite (a less well crystallized boehmite containing 1 7 H_2O/Al) are often completely transparent Heating causes dehydration and rearrangement leading to a series of transitional aluminas and finally α - Al_2O_3 A typical sequence of crystallization is the following [30]

$$AlOOH \xrightarrow{300\ C} \gamma - Al_2O_3 \xrightarrow{850\ C} \delta - Al_2O_3 \xrightarrow{1100\ ^\circ C} \theta - Al_2O_3 \xrightarrow{>1200\ C} \alpha - Al_2O_3$$

Boehmite gels consist of fibrillar or needle shaped crystals The surface area and pore size of several boehmite gels investigated by woltran [32] is listed in Table 1 6 The surface area of boehmite gel is quite sensitive to the H_2O Al ratio r used in gel synthesis procedure

Table 1 6 Characteristics of alumina gels prepared by controlled evaporation [30]

Gel	S_{BET} (m^2/gm)	d_{BET} (nm)	Porosity (%)
AlOOH[a]	275	7 2	40
AlOOH[b]	106	19	24
AlOOH[c]	163	12	30
AlOOH[d]	243	8 2	43

[a] Prepared from Al - sec - butoxide
[b] Prepared from Al - iso - propoxide
[c] 1% glycerol added
[d] Prepared using 0 05 g/lt submicron α - Al_2O_3 seeds

In boehmite the oxygens are arranged in a distorted octahedral configuration around aluminium and are organized in parallel layers linked by hydrogen bonds each layer of octahedra comprising two sublayers as shown in Fig 1 10

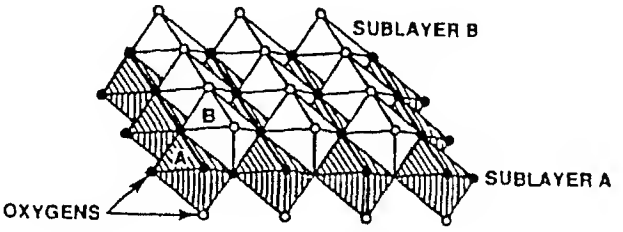

Fig 1 10 IDEAL BOEHMITE LAYER [30]

Upon heating boehmite gels exhibit a weight loss over the range 50 - 600 C due to the loss of structural and intercalated water and gradually transform to α - Al_2O_3 The topotactic transformation is accomplished by internal condensation of protons and hydroxyls between boehmite layers that removes half the oxygen from the layers causing a collapse and rearrangement of the oxygens into cubic close packing This and subsequent transformation to δ - and θ - Al_2O_3 at about 800 and 1000°C respectively are accompanied by a coarsening of microstructure as evidenced by a decreasing surface area and increasing pore size as shown in fig 1 10 and fig 1 11

According to Wilson and Stacey [33] and Wilson et al [34] the $\gamma \longrightarrow \delta$ transition represent the first step toward the ideal random distribution of vacancies on tetrahedral sites The c a ratio adjusts towards 1 the cubic value but concurrent ordering on the octahedral sites prevent the attainment of the cubic symmetry Their studies on macrocrystalline samples (> 1 μm)indicate the $\gamma \longrightarrow \theta$ conversion causes a decrease in the accessibility of planar hexagonally shaped pores that are formed parallel to the former < 010 > boehmite layers The topotactic $\delta \longrightarrow \theta$ transformation occurs by a rearrangement of Al cations within the cubic close packed oxygen array Wilson and Stacey (33) observed that θ - Al_2O_3 retains the same pore morphology as δ - Al_2O_3 but pore size increases from 6 - 10 nm [Fig 1 12] The $\theta \longrightarrow \alpha$ Al_2O_3 transformation occuring above 1100 C results from a reorganisation of oxygen into a denser hexagonal close packed configuration This is accomplished by a nucleation and growth process resulting in rapid coarsening of microstructure [Fig 1 11]

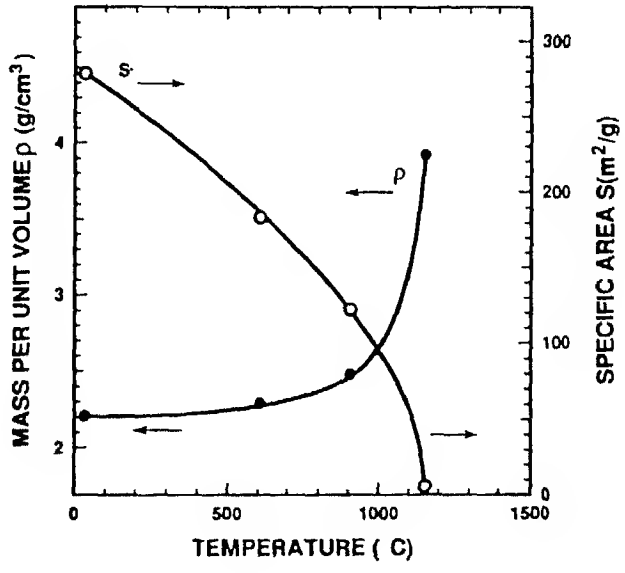

Fig 1 11 Density and specific surface area of boehmite xerogels after heat treatment (24 h) at the indicated temperatures [30]

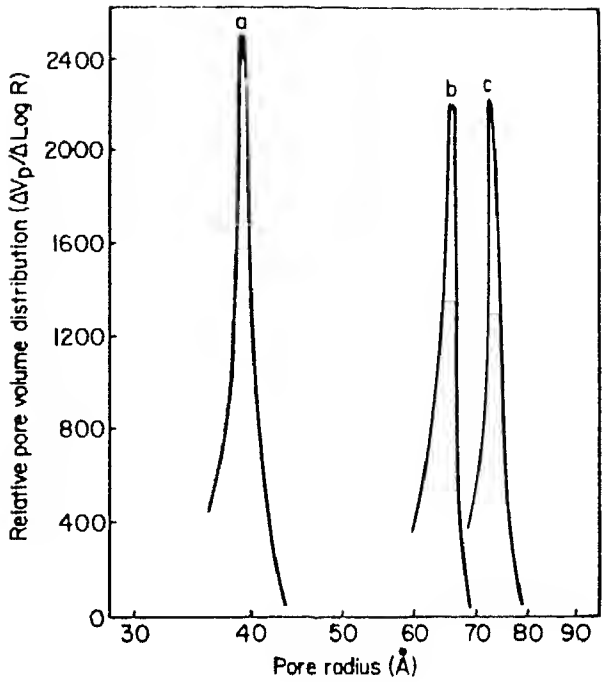

Fig. 1.12 Pore size distribution determined from desorption branches of N_2 isotherm. a) 500°C b) 900°C c) 1000°C . [30]

C. SOL - GEL DERIVED MEMBRANES.

The sol - gel route for the preparation of ultrafine grained ceramics was known for a long time. That the extremely narrow pores and pore size distribution of sol gel derived ceramics, obtained from uniform particle packing, is also one of the most desired microstructural property of membranes, was realized by Leenaars and Burggraaf in 1984.

Leenaars et al [10, 11, 12, 13] in a series of papers revolutionized the field of membrane research by synthesizing extremely stable γ - Alumina membranes with narrow pores and pore size distributions, capable of operation at elevated temperatures and pressures. Their pioneering work opened up yet another exciting field of sol - gel science.

Leenaars prepared alumina films (thickness < 20 μm) by a process in which a boehmite sol is successively gelled dried and calcined The resulting structure has the unique microstructural property of uniform and narrow pore size distribution

The flow diagram for the preparation of these unsupported membranes is shown in Fig 1 13

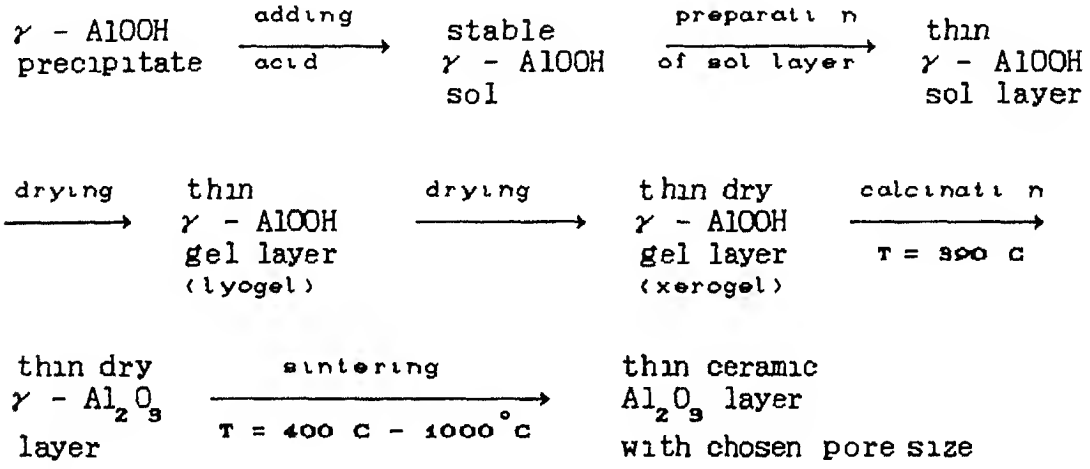

Fig 1 13 Flow diagram of preparation of alumina membranes

A series of membranes prepared containing 0 07 mol HNO_3 per mol of AlOOH heat treated at different temperature show the evaluation of various phases The crystallite size was calculated by X - Ray line broadening BET was used to characterize the pore sizes and surface area of the membranes The crystallite sizes are comparable with those found by electron microscopic measurements The table summarizing their results is shown

Table 1 7 Microstructural characteristics of membranes as a function of temperature treatment [10]

Temperature (C)	D_{hkl}	BET surface (m^2/gm)	Modal pore size cylindrical shape	Modal pore size slit shape	Porosity (%)
200	D_{120} = 6 2 D_{031} = 4 8	315	3 7	2 5	53
400	D_{400} = 6 4 D_{440} = 3 0	301	4 0	2 7	53
500	D_{400} = 6 4 D_{440} = 3 0	240	4 9	3 2	54
600	D_{400} = 6 4 D_{440} = 3 0	209	5 5	3 5	55
700	D_{400} = 6 4 D_{440} = 3 0	181	5 9	3 7	53
800	D_{400} = 6 4 D_{440} = 3 0	154	7 9	4 8	55

Leenaars explained the microstructure of the dried boehmite membranes as plate - shaped particles stacked in a card- pack structure This close - packed structure is the result of gel - compaction due to capillary forces during water extraction in the drying stage

While performing dipping experiments with supported membranes the main parameters that determined the formation of gel layer on porous supports are

1 Sol concentration

2 Dipping time

3 Pore size of support and

4 Type and amount of acid used to peptise the sol

It was found the tendency of gel formation increased with increasing sol concentration and dipping time and decreased with the pore size of support Also more massive sol particles formed by peptisation with increased acid additions as well as overaged sols lead to faster gel formation These results can only be explained if the formation of the klsupported top layer is thought to be as a slip - casting process Boehmite particles entering the pores of the supports clog them leading to an increase in sol concentration close to the support and ultimate gelation

The variation of thickness with dipping time show that the film thickness is proportional to the square root of dipping time further strengthening the slip - casting model Leenaars et al prepared membranes upto 8 μm thick on α - Al_2O_3 supports

The model suggested for slip casting [11] considers the pressure drop across the gel layer and the wet support as shown in Fig 1 14

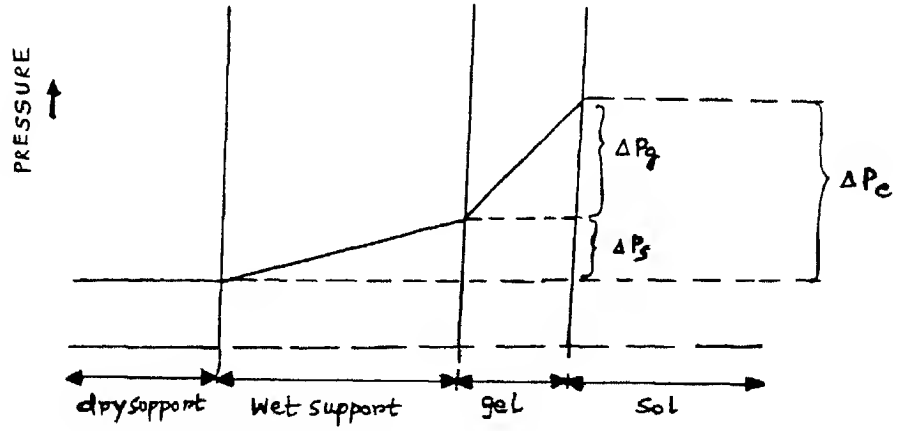

Fig 1 14 Pressure drop in a slip casting process [11]

Here ΔP_g = pressure drop over gel layer

ΔP_s = pressure drop over saturated support

ΔP_c = total drop = $\Delta P_g + \Delta P_s$

The thickness of the gel layer is given by

$$L_g = \left[\frac{2\ K_g\ \Delta P_g\ t}{\eta\ \alpha} \right]^{1/2} \qquad (1\ 3)$$

Where K_g = permeability constant of gel layer

$\alpha = \frac{\theta_s\ L_s}{L_g}$ θ_s = volume fraction of sol in support

η = viscosity of the sol

t = dipping time

Liquid flux through a cylinder under laminar flow conditions is given by the Poiseuille Formula

$$\frac{\Delta V}{\Delta t}\ \frac{1}{A} = \frac{R^2\ \Delta P}{8\eta L} \qquad (1\ 4)$$

Where $\frac{\Delta V}{\Delta t}$ is the volumetric flow rate

A is the flow area

R is the radius of the cylinder

ΔP is the applied pressure

η is the viscosity of permeant

L is the length of cylinder

The so called Kozney - Carman Equation describing laminar flow through a porous media is derived from 1 4 above

$$\frac{\Delta V}{\Delta t}\quad\frac{1}{A} = \frac{\Delta P\,\theta^3}{K\quad K_i\, L\,\eta\quad S_v^2\,(1-\theta)^2} \qquad (1\ 5)$$

Where θ = porosity

S_v = internal surface area

$K\ K_i$ = Kozney Carman constant

Leenaars (12) performed permeability experiments with supported alumina membranes He used different permeants The flux multiplied by viscosity of the solvents decreased in the order water hexane ethanol and S - butanol [Table 1 8]

Table 1 8 The volume flux of different permeants [12]

Permeant	Flux ($cm\ bar^{-1}\ hr^{-1}$)	Flux X viscosity ($cm\ bar^{-1}\ hr^{-1}\ cP$)
Water	Ø 54	Ø 63
Hexane	1 65	Ø 53
Ethanol	Ø 40	Ø 50
S -butanol	Ø 11	Ø 38

The decline of flux X viscosity (a measure of K) with η can be explained by the size effect of the permeant molecules provided adsorption takes place

The Kozney Carman constant was calculated to be 13 3 $\pm$ 2 The high value can be explained by the card pack structure of plate shaped crystallites The MWCO of these membranes were dependent on the calcination temperature For membranes calcined at 400 C it was 2000 Daltons and for

800 C it was 200 000 Daltons

Larbot et al [22] prepared TiO_2 and ZrO_2 membranes by the sol gel route The thickness of these membranes were found to be linearly varying with the square root of time The reported the relation $L = 0\ 57 \sqrt{t}$ where L is the membrane thickness and t is the deposition time for titania membranes and $L = 1\ 4 \sqrt{t}$ for zirconia membranes The anatase ⟶ rutile conversion is TiO_2 membranes at ≃ 600 C has to be carefully controlled to prevent cracking of the membrane top layer The pore size of membranes treated at higher temperatures were found to be greater In titania membrane pore size variation was from 3 to 180 nm with increasing temperature The corresponding values for ZrO_2 membranes was 3 to 80 nm [Fig 1 15]

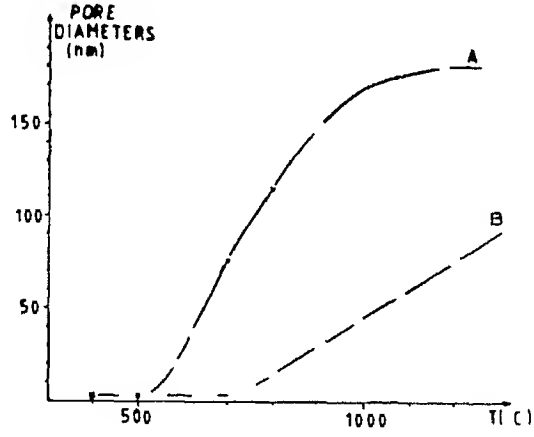

Fig 1 15 Pore diameter as a function of sintering temperature

A) TiO_2 membranes B) ZrO_2 membranes [22]

Water permeability tests were carried out the water flux was found to very nonlinearly with pressure It increases greadually then levels off at high pressures Permeability was found to be a function of pore diameter as well Fig 1 16(a) and 1 16(b)

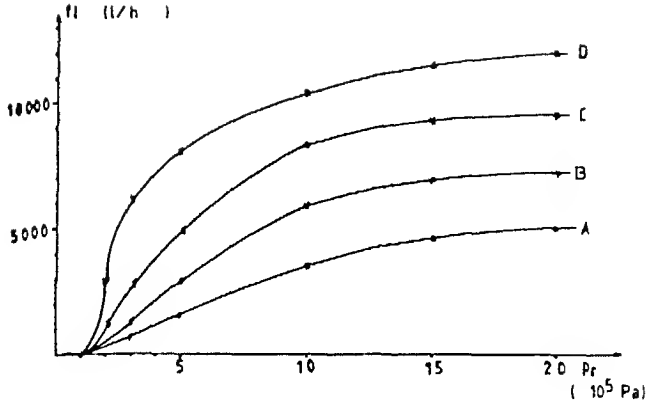

Fig 1 16(a) Flux through titania membranes pore diameter A) 3 B) 20 C) 75 and D) 180 nm [22]

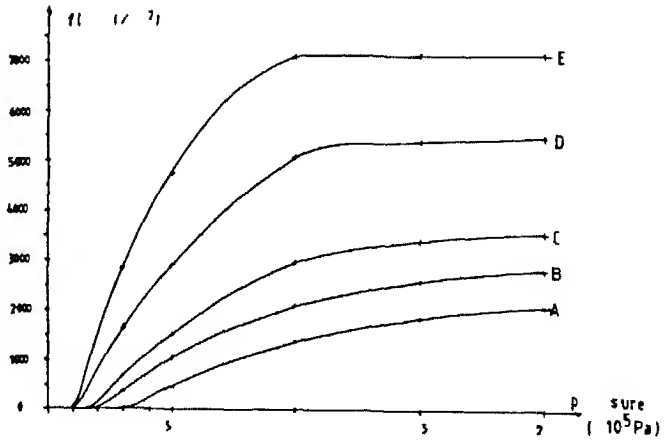

Fig 1 16(b) Flux through ZrO_2 membranes pore diameters A) 3 B) 10 C) 20 D) 50 and E) 85 nm [22]

Lin et al [23] reported the preparation of a high temperature thermally stable Al_2O_3 membrane using a La doped boehmite sol He reported the addition of PVA and proper aging of the sol to prepare crack - free top layers He checked the extent of microcracking in the top layer by gas permeation measurements

For homogeneous porous disk and pure non -adsorbable gas the gas permeability can be correlated the average pressure across the disk (P_{av}) by

$$F/L = \alpha + \beta P_{av}$$

where

$F = QL/S \ (P_h - P_l)$

Q = Volumetric gas flow rate

L = disk thickness

S = permeation area

P_h P_l = high and low pressure sides of disk

Here α is the coefficient due to knudson flow

and β is the coefficient due to viscous flow

For a membrane free from microcracks the flow should be knudsen type and hence pressure independent Thus this pressure independency of permeability can be checked as evidence of crack free membranes

Similar results were obtained by Uhlhorn et al for alumina membranes [23] They developed a method of repairing microcracks by multiply dipping With increase in the number of coatings the slope of he permeability vs average pressure slowly decreased [Fig 1 17]

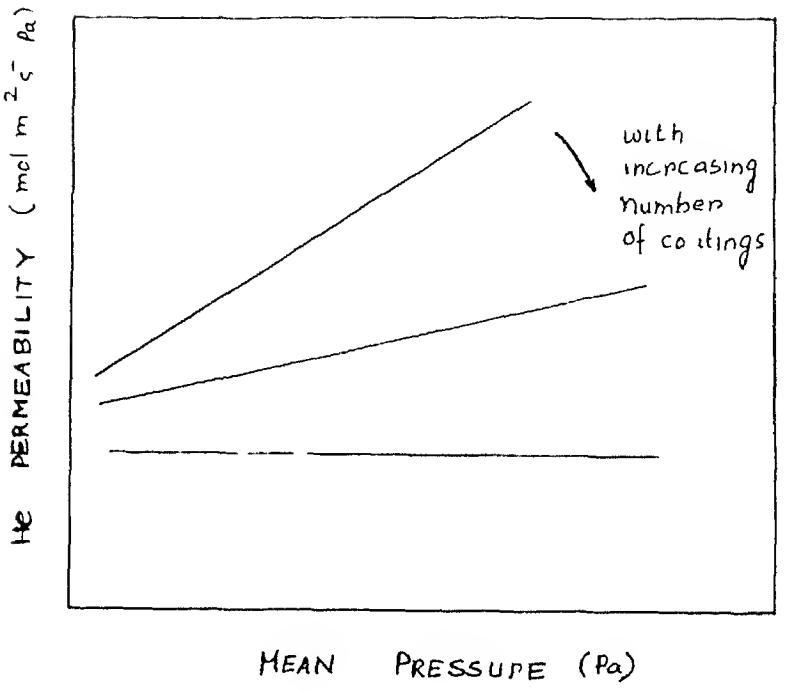

Fig 1 17 Schematic representation of the change in slope of permeability vs mean pressure Pressure independency shows a membrane free from microcracks

Uhlhorn et al (23) also measured the water permeability of their γ - Al_2O_3 membranes The water flux was found to vary linearly with applied pressure [Fig 1 18]

The solute retention (SR) of membrane for organic molecules of known molecular weight is defined as $SR = 1 - C_p / C_f$ where C_p and C_f are the solute concentration in the permeate and feed respectively

Leenaars et al [13] measured the solute retention of Al_2O_3 membranes with different molecular weights of PEG (polyethylene glycol The resultant sigmoidal curve is shown in Fig 1 19 The MWCO values when SR = 90% can be calculated from these curves

Zaspals et al (24) prepared alumina and titania binary membranes by dipcoating supports in binary sols prepared by mechanically mixing TiO_2 and Al_2O_3 sols Mean pore diameters were 4 5 nm and 3 nm for TiO_2 and Al_2O_3 membranes respectively and 3 7 nm for binary membranes The destructive nature of the anatase $\longrightarrow$ rutile transformation could be retarded by carrying out hydrolysis of titanium tetra - isopropoxide in the presence of SO_4^{2-} ions Titania membranes have a lower tortuosity value than alumina membranes in accordance to the difference in particle morphology

Hisich et al [25] prepared microporous alumina membranes by the sol gel technique and also characterized the available tubular microfiltration modules by the permeability tests Crossflow membrane filtration was utilized The rejection characteristics as well as gas permeation experiments were done to evaluate the separation factors and the viability of these modules in industrial applications

Huis in't Veld et al [26] used the so - called reservoir method to hydrolyse magnesia and change the chemical nature of the pores in a γ - Al_2O_3 membrane The MgO concentrations were about 40% This gave < 1 nm sized pores which gave very good results in gas separation experiments

Lin et al [27] used a novel CVD method to modify membrane pores A solid oxide (YSZ) is first deposited on the internal walls of the membrane The deposit is the product of two vapour reactants introduced from both sides of the membrane

After the membrane pore is closed by CVD a thin solid oxide electrolyte film can grow on one side of the membrane via EVD

W Van Praag [28] prepared Al_2O_3 - TiO_2 binary membranes by a sol - gel technique and modified them by impregnating Ag or V_2O_5 After impregnation the pore diameter measured by BET remained the same while

porosity and permeability decreased This can be explained by constricted membrane pores

Yamaki et al [29] used ultrafine zirconia particles prepared by the reverse micelle method to control the pore characteristics of alumina membranes The idea was to develop permselective membranes for separation of small molecular size gases Ultrafine zirconia particles were formed by the hydrolysis of zirconium tetrabutoxide in micro water pools of reversed micelles formed with a novel surfactant dioelyl phosphoric acid (DIKOA) Repeating the dipping calcination cycles the mesopores of the α - Al_2O_3 support tubes were packed with zirconia particles

The gas permeability of these modified membranes decreased with increased dipping firing cycles The separation factors of hydrogen to nitrogen achieved was 3 4 which was lower than the knudsen value of 3 74

2 STATEMENT OF THE PROBLEM

The field of inorganic membranes is dominated by ceramic ultrafiltration and microfiltration membranes The membranes that are commonly available are generally of the asymmetric composite variety with a thin film of γ-Al_2O_3 ZrO_2 TiO_2 etc on an α-Al_2O_3 support The membranes have narrow pore sizes and pore size distributions The thickness of the membrane is directly related to the membrane resistance to fluid flow - thin membranes give high flux values

The aim of this present work is to prepare asymmetric composite membranes of γ-Al_2O_3 on α-Al_2O_3 supports by using a sol-gel method This involves the following steps (i) Preparation of the α-Al_2O_3 support with suitable pore size distribution (ii) Preparation of a boehmite sol for depositing the membrane on substrate (iii) Deposition of membranes of various thickness on the substrate (iv) Heat treatment of the composite membranes to yield desired pore size and pore size distribution (v) Characterization of the membrane (vi) Measurements on the membranes with a view to find their suitability for various applications

This work aims to study each of these steps with a view to learn and optimize the techniques of preparation of composite ceramic membranes

3 EXPERIMENTAL PROCEDURES

3 1 Preparation of the substrate

The first step in the preparation of supported γ - Al_2O_3 membranes was the preparation of α - Al_2O_3 supports (also called the substrates) These substrates need to be sufficiently porous to allow fluid flux through itself on the other hand they must have sufficient strength to withstand high pressures in permeation

After reviewing the available literature it was decided that the supports must have the following properties

A) A total porosity of 40 - 50%

B) Total porosity = Open porosity

C) Pores of around 1 μm diameter

D) A narrow pore size distribution

E) Moderate strength

Keeping in view the above a series of sintering experiments were carried out to prepare pellets of α - Al_2O_3 by the traditional ceramic powder pressing route

Al_2O_3 powder (AKP - 50 Sumitomo Chemical Co Japan) average particle size 0 3 μm and maximum impurity of 0 01 % was used

The Al_2O_3 powders were dry pressed without any additives in a hydraulic press using high chromium die steel moulds into pellets of 25 4 mm diameter and 3 mm thick The pressure was slowly applied to reach a maximum pressure of 116(MPa) (6 ton load) It was maintained for 30 seconds to ensure proper homogenisation and then the pressure was slowly released to reduce the chances of spring-back and subsequent lamination/cracks It was found that the quality of the as pressed pellets is a strong function of the moisture content of the powders as well as of the atmosphere Since no PVA or any other additive were used to ensure better flow properties while pressing utmost care was taken to press the green pellets The powders were usually oven dried

and pressed while hot

Sintering was done in Lemont high temperature furnace (Lemont KRXV - 2) made by Lemont Scientific Inc Boalsburg U S A First the samples were heated in air at a heating rate of 3 5 C/min till 620 C then at 6 C/min till the desired temperature It was held at the maximum temperature for 1 hr and then cooled at 3 5 C/min to room temperature

Initially four temperatures were chosen for sintering 1400 C 1300 C 1200 C and 1100 C After density and porosity measurements by Archimede s principle and keeping in mind the requirements of the support pellets sintered at 1100 C / 1 hr were chosen as the right candidate for membrane supports All further supports were therefore made by sintering the pellets at the above mentioned temperature

After sintering the pellets were polished with SiC (800 grit) and finally with AKP - 50 Al_2O_3 powders to ensure a smooth surface for coating They were then ultrasonicated in acetone medium dried and stored for further use

3 2 Preparation of the composite membrane

3 2 1 Sol preparation

The reagents used for the preparation of boehmite sol by the Yoldas method were

A) Aluminium - sec - butoxide [Alfa Products] $Al(OC_4H_9)_3$ F W 246 32

B) Propan - 2 - ol [S D Fine Chem Ltd Boisar] $(CH_3)_2CHOH$ F W 60 10

C) Nitric Acid (Conc) [S D Fine Chem Ltd , Boisar] HNO_3 F W 63

D) Triple distilled water

The molar ratio of the different ingredients were as follows

Al - sec - butoxide	Water	HNO_3
1	150	0 07

Since Al - sec - butoxide is very hygroscopic and undergoes immediate gelation in contact with atmospheric moisture the sol was prepared

in a controlled atmosphere Glove Box [Labconco Corporation] To facilitate easy handling of alkoxide it was mixed with Propan - 2 -ol (1 1 weight ratio)

First the weighed amounts of Al - sec - butoxide and propan - 2 -ol were mixed inside the glove box with the help of a magnetic stirrer in a beaker covered with an aluminium foil The correct molar amount of triple distilled water was weighed out in a separate beaker This beaker was also securely capped and the water was heated in an oil bath maintained at a temperature of 85 C The thermometer was kept in such a way that it recorded the correct temperature of the water This is very important because hydrolysis of Al - sec - butoxide at higher temperatures (> 80 C) yields boehmite whereas cold water hydrolysis yields bayerite a hydroxide incapable of conversion to any of the transition aluminas (γ - δ - θ - etc)

The Al - sec - butoxide - propan - 2 - ol mixture was then transferred outside the Glove box and added dropwise to the water (heated to 85 C) under vigorous stirring A white precipitate of $Al(OH)_3$ immediately forms The slurry is kept in stirring condition for about 45 mins After that conc HNO_3 is added dropwise to the slurry at 85 C The precipitate redissolves and a clear sol results The sol is kept in a covered beaker and stirring is continued for another hour to facilitate complete peptization Then the sol is transferred to a round bottom flask and kept under reflux condition at 80°C overnight

The resulting clear sol is filtered through a Ø 22 μm filter (Millipore Co U S A) and stored in air tight bottle in a desiccator

3 2 2 Determination of sol concentration

A known amount of the sol prepared by the method described in the last section is transferred to a previously cleaned, dried and weighed empty Platinum crucible The sol is transferred volumetrically by a 1 ml pipette The platinum crucible is covered by a lid and heated in a furnace

till 1200 C at the rate of 5 C/min It was held at 1200 C for 3 h and then cooled at 5 C/min

The platinum crucible was again weighed after it has cooled down to room temperature The total weight of the platinum crucible and the solid residue of the sol was noted The weight of the platinum crucible was subtracted to find the solid residue of the sol The solid powder was checked by XRD and was found to be composed of α - Al_2O_3 This way the amount of Al_2O_3 (in gms) per unit volume of the sol was found out It was converted to convenient units of moles of boehmite/litre

3 2 3 Dipping Experiments

The composite membranes were formed by dip coating the supports in the sol and subsequent heat treatment

The dip coating technique involved bringing a porous support in contact with the sol for a few seconds so that a coating of sol particles is formed on one side of the support The sol particles are initially sucked inside the pores and deposited on the walls This lead to pore clogging and ultimate gel formation

The whole process is shown schematically in Fig 3 1

The support was held firmly by a tweezer so that its surface is parallel to the sol surface in the beaker After allowing the required time of contact the whole system is whisked up so that the substrate leaves up the sol surface at an acute angle This minimizes thickness variations over the substrate as the last drop of the sol adhering to the substrate is brought to the very edge and is wiped away cleanly with tissue paper

The above process led to samples with fairly homogeneous layers with albeit small variations in thickness

To study the effect of dipping time on the coating thickness, samples were prepared by dip coating for various times 10 seconds 20 seconds 30 seconds and 90 seconds Then they were calcined at 600 C / 3h The membrane

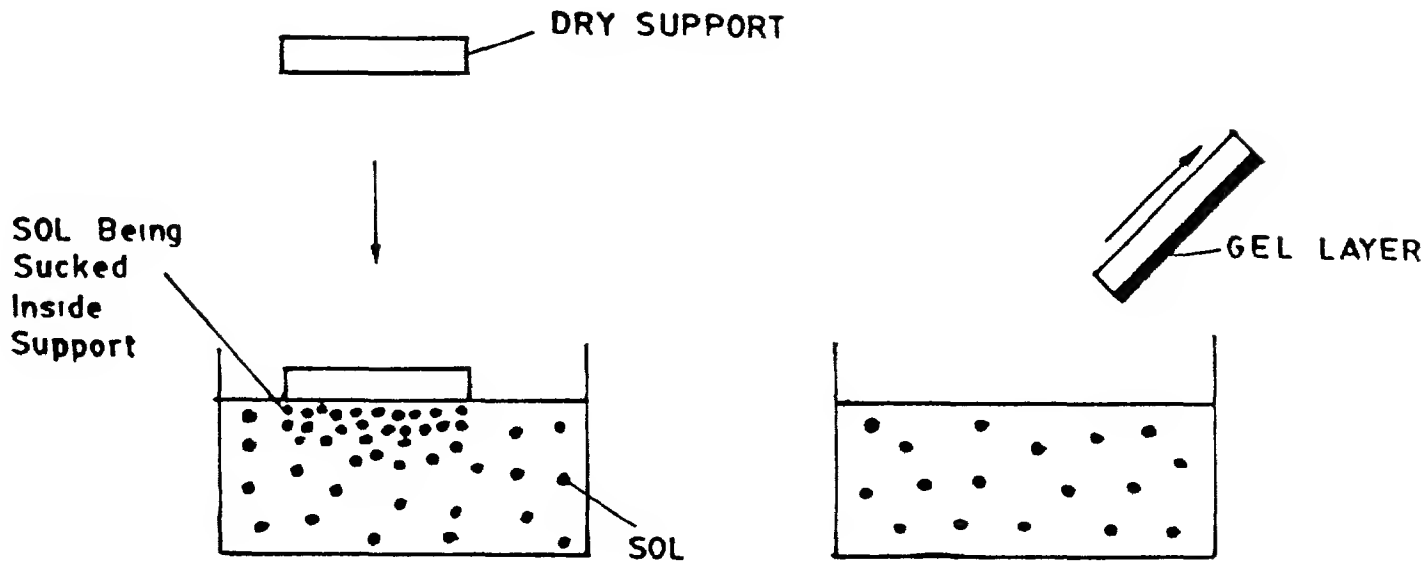

Fig 3 1 Schematic diagram showing the dip coating process

samples were then broken and the fracture surface seen under a JEOL Scanning Electron Microscope (JSM 840 A Japan) The thickness of the membranes were difficult to measure accurately from the SEM photographs because of small variations in thickness as well as an absence of a well defined boundary between the membrane and the substrate So an approximate outline of the membrane layer was traced out on a graph paper and its area was determined This divided by the length of the photograph gave the thickness of the membrane The thickness was then plotted against square root of the dip coating time

3 2 4 Heat treatment of membranes

After depositing the top layer the sample was left in covered petri dish in the desiccator for slow drying of the gel layer The usual drying times were about 12 hrs

The samples were then calcined in a horizontal tube furnace employing SiC heating elements The heating rates employed were very slow Fast heating rates have led to cracks in the top layer The calcination was done according to the following schedule The samples were heated at 1°C/min till 120 C It was held at that temperature for 30 minutes to remove most of the adsorbed and constitutional water Then the heating rate was 2°C/min till the maximum temperature where the samples were held for 3 hrs before cooling off at 2 C/min to room temperature

Four temperatures were chosen and membranes calcined at those temperatures for 3 hrs were prepared Thus the different samples were

500 C/3hr 600 C/3hr 700 C/3hr & 800°C/3hr samples

3 3 Characterization techniques

3 3 1 Density and Porosity measurements of the supports by Archimede s Principle

The test samples were dried thoroughly at 140 C for 12 hrs The dry weight (W_d) of the samples were taken using an electronic balance (Afcoset

ER 1200 A) The samples were suspended in distilled water in a beaker and evacuated for about 2 hrs by keeping in a vacuum desiccator and with a vacuum system The weight of the evacuated samples with water penetrated in the open pores was taken while suspended in water (W_2) Immediately after the samples were removed from water blotted lightly with a wet tissue paper and the weight taken in air (W_3) The sintered density was calculated from the following formula

$$\text{Sintered density } (\rho_s) = \frac{W_1}{W_3 - W_2} (\rho_w - \rho_{air}) \qquad (3\ 1)$$

where ρ_w = density of water

ρ_{air} = density of air

The porosities were calculated using the following formulae

$$\text{True Porosity} = \left[1 - \frac{\rho_s}{\rho_{th}} \right] \times 100\ \% \qquad (3\ 2)$$

$$\text{Open Porosity} = \frac{W_3 - W_1}{W_3 - W_2} \times 100\ \% \qquad (3\ 3)$$

where ρ_{th} is the theoretical density of Al_2O_3

3 3 2 Measurement of fracture strength of the supports

Fracture strength was measured by the three point bending test The samples of the substrates (1100 C/1h) were cut using a low speed saw [Isomet (Buehler)] with a diamond blade of thickness 0 3 mm The size of the samples were approximately 15 mm X 2 mm X 0 8 mm All the sides of the samples were polished with 400 grit SiC powder on glass plate Fracture strength was measured for all samples using an Instron 1195 system A 1000 kg load cell was used with cross head speed of 0 2 mm/min The span used was 6 3 mm Full scale load and chart speed were 2 kg and 50 mm/min respectively

The fracture strength was calculated by using the following formula [37]

$$\text{Fracture Strength} = \frac{1\,5\ PL}{bh^2} \quad \text{MPa} \qquad (3\,4)$$

where P = Fracture load in kg

L = Span in mm

b = Width of the specimen in mm

h = Depth of the specimen in mm

3 3 3 Mercury Porosimetry

The Washburn equation [38]

$$\Delta P_r = -2\gamma \cos\theta \qquad (3\,5)$$

is the basis of mercury penetration porosimetry work Here

ΔP is the pressure differential across the mercury interface in a pore

r is the radius of the pore

γ is the surface tension of the mercury

θ is the contact angle for the mercury - solid interface

The experimental method employed in mercury porosimetry involves the evacuation of all the gas from the volume containing the sample Mercury is then forced into the inter particle voids and intra particle pores A means of monitering both the applied pressure and the intruded pressure are integral parts of all mercury porosimeters During pressurization the calibrated penetrometer measures the intruded volume into pores of progressively smaller radii with increasing pressure During depressurization the opposite happens and the extrusion curve is obtained

From the intrusion - extrusion curves a number of physical parameters can be determined e g solid compressibility surface area of the sample and its pore size distribution

The pore size distribution Function $D_v(r)$

When the radius of a cylindrical pore is changed from r to r − dr the corresponding decremental change in pore volume V is

$$dV = -2\pi r l\, dr$$

where n = no of pores of radius r and length l

When pores are filled according to Washburn equation the volumetric change with decreasing radius does not necessarily decrease since it corresponds to the filling of a new group of pores

Thus when the pore radius into which intrusion occurs changes from r to r − dr the corresponding volume change is given by

$$dV = -D_v(r)\, dr \text{ where}$$

$D_v(r)$ is the volume pore size distribution function defined as the pore volume per unit interval of pore radius

Differentiating Washburn equation assuming constancy of γ and θ

$$Pdr + rdP = 0$$

$$dV = D_v(r)\,\frac{r}{P}\,dP$$

$$\text{or} \quad D_v(r) = \frac{P}{r}\left[\frac{dV}{dP}\right] \qquad (3\ 6)$$

The mercury porosimetry study was done with an automatic porosimeter (Micromeritics Poresizer) under the following operational parameters

Penetrometer volume	5 2974	ml
Advancing contact angle	130	degree
Receding contact angle	130	degree
Mercury surface tension	485	dyne/cm
Mercury density	13 5335	g/ml

The supports were directly introduced inside the pressure chamber and the system pressurized After the maximum pressure has been

applied corresponding to the filling of the smallest size pores the system was depressurized The pore size distribution function was calculated from the intrusion - extrusion curve It was plotted against the pore diameter

3 3 4 Nitrogen adsorption - desorption

Adsorption studies leading to measurements of pore size and pore size distributions generally make use of the Kelvin Equation [38] which relates the equilibrium vapour pressure of a curved surface such as that of a liquid in a liquid in a capillary or pore to the equilibrium pressure of the same liquid on a plane surface

$$\ln \frac{P}{P} = - \frac{2\gamma \bar{V}}{rRT} \cos\theta \qquad (3\ 7)$$

where P is the equilibrium vapour pressure of the liquid contained in pore of radius r and P is the equilibrium pressure of the same liquid exhibiting a plane surface The terms γ and $\bar{V}$ are the surface tension and the molar volumes of the liquid respectively and θ is the contact angle with which the liquid meets the pore wall

In a pore wall the overlapping potentials of the walls more readily overcome the translational energy of an adsorbate molecule so that condensation will occur at a lower pressure in a pore than that normally required on an open or plane surface Thus as the relative pressure is increased condensation will occur first in pores of smaller radii and will progress into larger pores until at a relative pressure of unity condensation will occur on those surfaces whose radius of curvature is essentially infinite Conversely, as the relative pressure is decreased evaporation will occur progressively out of pores with decreasing radii

The adsorption studies were done on Quantasorb Sorption System (Quantachrome Corporation U S A) using nitrogen as the adsorbent and helium as the carrier gas

Samples for nitrogen – adsorption - desorption studies were prepared in the following manner Bars of 10 mm X 3 mm X 3 X mm were cut from the support samples They were then polished thoroughly with 800 grit SiC powder and ultrasonicated This type of sample configuration was chosen because it would fit the standard U – tube holder that was available with the Quantasorb System The porous support bars were degaussed at 300°C for 8 hrs before measuring their surface area Next the porous supports were dipped in the prepared boehmite sol and then calcined at different temperatures viz 500 C 600 C 700 C 800 C for 3 hrs The surface area and average pore diameter of the samples were determined at relative nitrogen partial pressures of 0 3 and 0 95 The total surface area of the support was subtracted from that of the support with membrane material to get the total surface area of the membrane only It was divided by the mass of the membrane material to get the specific surface area

The single point BET method was employed to find the surface area The partial pressure of N_2 was adjusted by controlling the flow rate of N_2 and He The desorption signal was used because it generally gave a Gaussian curve Pure N_2 was used to calibrate the signal Calibration volume was 1 ml at attenuation 32 and 180 mA filament current

The total surface area (S_t) by the single point BET is given by

$$S_t = \left(1 - \frac{P}{\bar{P}}\right)\left(\frac{A}{A_c}\right) V_c \left(\frac{N A_{cs} P_a}{RT}\right) \qquad (3\ 8)$$

where $\frac{P}{\bar{P}} = 0\ 3$

A/A_c is the ratio of desorption to calibration signal

V_c is the volume of calibration

N is the Avagadro Number

A_{cs} is the cross sectional area of adsorbate molecule

P_a is the ambient pressure

R is the Gas constant and

T is the temperature of ambient

The pore volume is the total amount or adsorbate adsorbed at Ø 95 partial pressure of the adsorbate This is the so called Gurvitsch rule Assuming cylindrical geometry the average pore diameter can be determined

$$d = \frac{A}{A_{cal}} \times V_{cal} \times \frac{P_a \times V_m}{RT} \times \frac{4}{S_t} \times 10^4 \text{ Å} \quad (3\ 9)$$

where A/A_{cal} has the same meaning but measured at Ø 95 partial pressure

and V_m is the molar volume of N_2 (= 34 7 cm^3)

3 3 5 X - Ray Diffraction

X - ray diffraction patterns (2Θ vs intensity) of powder samples were taken with Reich - Seifert Iso - Debyeflex 2002 diffractometer using CuKα radiation (λ = 1 5418 Å)

X - ray analysis was carried out on the following samples

a) Powder gel samples calcined at 300 C 400 C 500°C 600 C 700°C 800 C 900 C and 1000 C to see the phase evolution of transition aluminas

b) Supported membranes calcined at 600°C/3h

The X - ray diffraction plots of the samples were measured in 2Θ range of 10 to 72 for phase detection in powdered samples and 42 to 48° for phase detection in supported membranes

The d values were calculated using the Bragg s condition

$$2d \sin\theta = n\lambda \quad (3\ 10)$$

where n = order of reflection

λ = the wavelength of radiation

d = the interplanar spacing

θ = the diffraction angle

The d values so obtained were compared with ASTM standards to identify the phases present

Operational parameters for X – Ray Diffraction

	For powdered samples(gel-derived)	For supported membranes
Current voltage	20 mA 30 kV	20 mA 30 kV
Time constant	10 s	10s
Beam slit width	2 mins	2 mins
Detector slit width	0 3 mm	0 3 mm
Scan speed	3 /min	0 6 /min
Chart speed	3 cm/min	1 2 cm/min
Counts per minute	5 K	2 K

3 3 6 Thermal Analysis

3 3 6 1 Differential Thermal Analysis (DTA)

Any phase transformation or chemical reaction accompanied by absorption or evolution of heat can be readily detected by DTA For the present investigation a Shimadzu Model DTA was used Platinum crucible was used to hold the sample and the reference (α - Al_2O_3 in this case)

The samples for thermal analysis (DTA and TGA) were prepared in the following manner Alumina sol prepared by the process described in Section 3 2 1 was left in the oven to gel at 80 C in a covered petri dish After 48 hrs it formed a monolithic mass This was then crushed in an agate mortar into a fine powder DTA was done on this powder heating it from room temperature to 1200 C The rate of heating was kept at 10°C/min The endothermic and exothermic peaks corresponding to a temperature difference (ΔT) between the test sample and the reference and signifying a chemical reaction taking place were used to characterize the phase transformation pathway of boehmite gels

3 3 6 2 Thermogravimetry (TG)

The amount of weight loss and its rate for a sample heated progressively to higher temperatures are effective means of understanding

solid state reactions The technique known as thermogravimetry was employed for boehmite gels prepared by Yoldas method (section 3 2 1) The powdered gels were packed into a platinum crucible which was hung by a platinum wire inside a vertical coil wound furnace The weight loss was recorded by an electronic balance [Afcoset ER 1200 A (correct upto 0 0001 g)] The sample was heated at 10 C/min till 1000 C The corresponding weight loss vs temperature data was recorded

3 3 7 IR Studies

The vibrational motions of the chemically bound constituents of matter have frequencies in the infrared regime The oscillations induced by certain vibrational modes provide a means for matter to couple with an impinging beam of infrared electromagnetic radiation and to exchange energy with it when the frequencies are in resonance In the infrared experiment the intensity of a beam of infrared radiation is measured before (I_0) and after (I) it interacts with the sample as a function of light frequency (ν) A plot of I/I_0 versus wave number ($1/\nu$) is the infrared spectrum The identities surrounding environments and concentration of the chemical bonds present can be determined

IR samples were prepared with powders prepared as in Sec 3 3 6 1 and calcined at 200 C 400 C and 600 C An as-dried powder was also taken The powders were mixed with KBr and pressed into small pellets (1 1 cm ϕ) with a steel die The reference sample was a pure KBr pellet The instrument make was Jasco Corporation (Japan)

The plot of I/I_0 vs wave number showing the progressive removal of organic groups in gel derived boehmite powder with increasing temperature was obtained

3 3 8 Scanning Electron Microscopy

The microstructure of the membranes were studied with a JEOL scanning electron microscopy (JSM 840 A Japan) In the present investigation

the fracture surface of the composite membrane was seen in the secondary electron emission (SE) mode Also the surface structure in a free standing membrane film was also seen The free standing membranes were prepared by leaving the sol in a polypropylene dish in a desiccator overnight for flake formation They were then calcined at 650 C for 3 hrs

Before viewing under SEM the samples were sputtered with silver in a coating unit

3 3 9 Water Permeability Tests

To measure the permeability of the supported membranes to liquids membranes were subjected to water permeation tests For that a special cell was designed [Fig 3 2] The cell was fitted to an ultrafiltration permeation system [Fig 3 3] The system employed was the unstirred mode ultrafiltration ie unsteady state

The flow of water through the membrane can be understood by the Kozney Carman Relationship for liquid permeation

$$\frac{\Delta V}{\Delta t A} = \frac{\varepsilon^3}{K \eta S^2 (1 - \varepsilon^2) L} \Delta P \qquad (3\ 11)$$

Here ΔV is the volume of water permeability

Δt is the time required

A is the available membrane permeation area

ε is the porosity of membrane

L is the thickness of the membrane

S is the surface area /unit volume of solid material

and K is the Kozney Carman constant

This equation is in fact the Poiseule equation for viscous flow adapted for a porous medium

Membrane samples calcined at 500 C 600 C 700 C and 800 C were used for measuring the water permeabilty Membranes were inserted in the cell and the system was pressurized The first reading was taken after the system

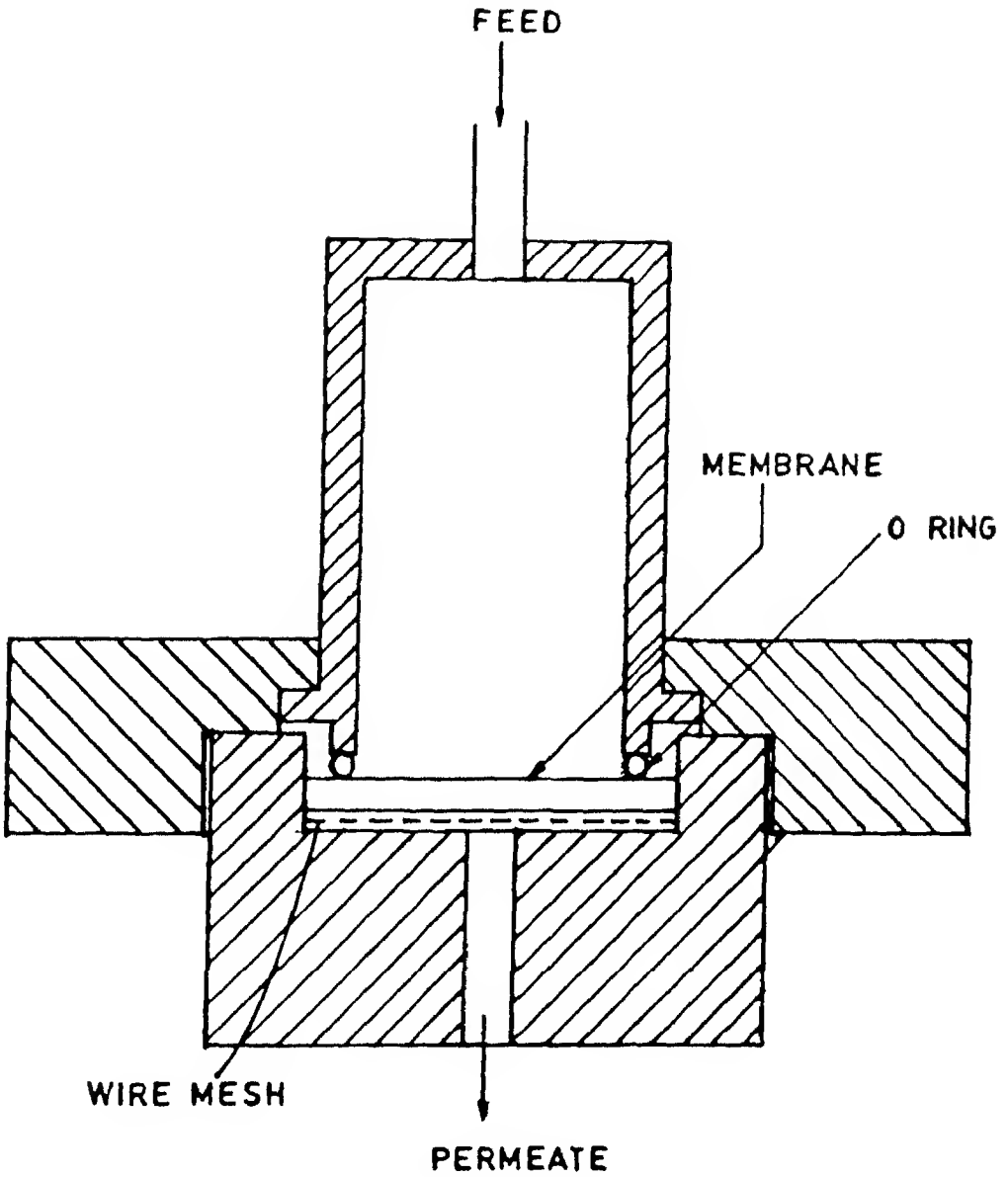

Fig. 3.2 Cross sectional view of the unstirred ultrafiltration cell

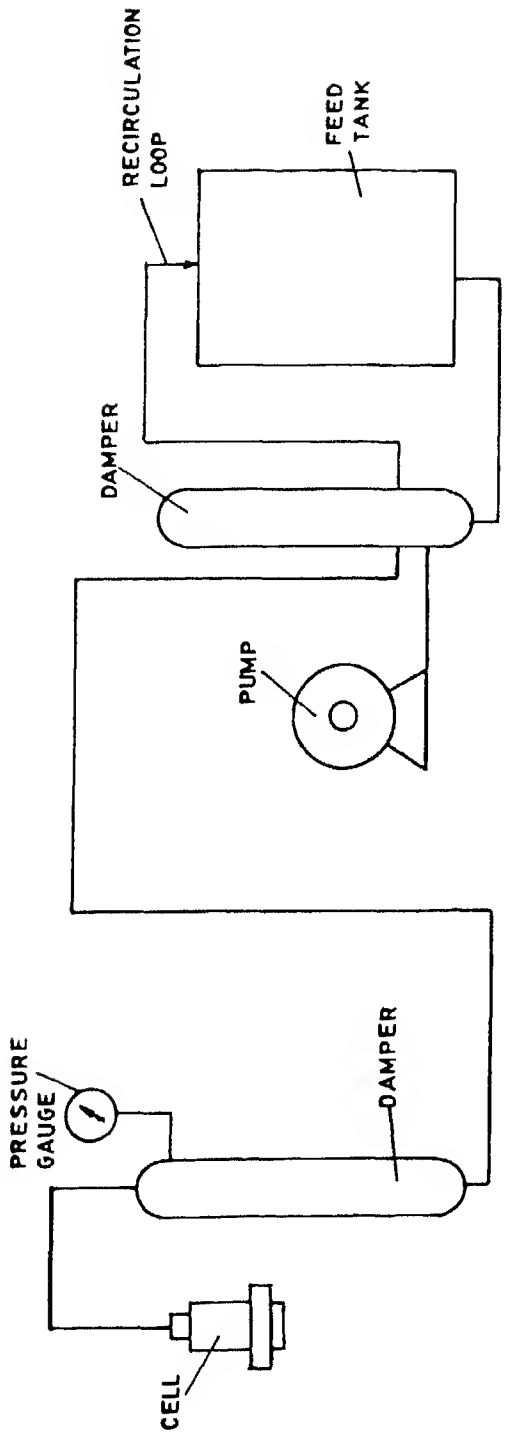

Fig 3.3 Schematic diagram of the ultrafiltration set up

has stabilized at 100 psi A total of three readings were taken at each pressure setting over different time intervals The volume that was collected over a given time interval was divided by the area (3 142 cm^2) of the membrane and the time taken to get the flux Similarly the water flux was measured at 150 200 and 250 psi A plot of water flux vs transmembrane pressure was made for each membrane The Kozney Carman constant can thus be determined knowing the porosity and interval surface area of the membrane

3 3 10 PEG Permeation and Retention Tests

The passage of large organic macromolecules through membranes is used to characterize the membrane itself In our study we used polyethylene glycol M W 4000 [Fluka] and polyethyleneglycol M W 6000 [S D Fine Chem] to study the flux decline behaviour and rejection characteristics of Al_2O_3 membrane

The same cell and unstirred mode ultrafiltration system was used At the very beginning calibration curves of refractive index vs concentration were made for both PEG 4000 and PEG 6000

Solutions of 0 0 5 1 2 and 4 wt % PEG were made for both the molecular weights Their refractive index was measured by a refractometer (Bausch & Lombe)

For rejection studies a 1 wt % solution of the PEG was made the feed solution The pressure chosen was 150 psi The membranes were inserted and the system was pressurized After the pressure had stabilized the permeate was collected and its refractive index checked The corresponding value of the concentration was obtained from the calibration curve

Solute rejection (SR) is defined as

$$SR = \left[1 - \frac{C_p}{C_f}\right] \quad X \quad 100\% \qquad (3\ 12)$$

where C_f = concentration in feed stream

C_p = concentration in permeate stream

Thus the rejection values for all the membranes for both the PEG varieties were measured

The flux decline characteristics of the membranes (500 600 700 800) were investigated using PEG 4000 A 1 wt % solution of PEG 4000 was chosen as the feed The chosen pressure was 150 psi The flux of the permeate was measured at regular time intervals The duration of the PEG runs were 120 minutes During this time the decline of flux through the membrane due to concentration polarization was observed

Concentration polarization usually occur in unsteady state ultrafiltration due to the building up of rejected species at the membrane surface This results in an increase in osmotic pressure of the feed solution close to the membrane surface and a reduction in the driving force for ultrafiltration The flux equation can be written as

$$J = \frac{(\Delta P - \Delta \pi)}{(R_m + R_p)} \qquad (3\ 13)$$

where R_m is the resistance due to the membrane

R_p is the resistance due to the polarization

$\Delta \pi$ is the osmotic pressure difference that builds up due to solute rejection

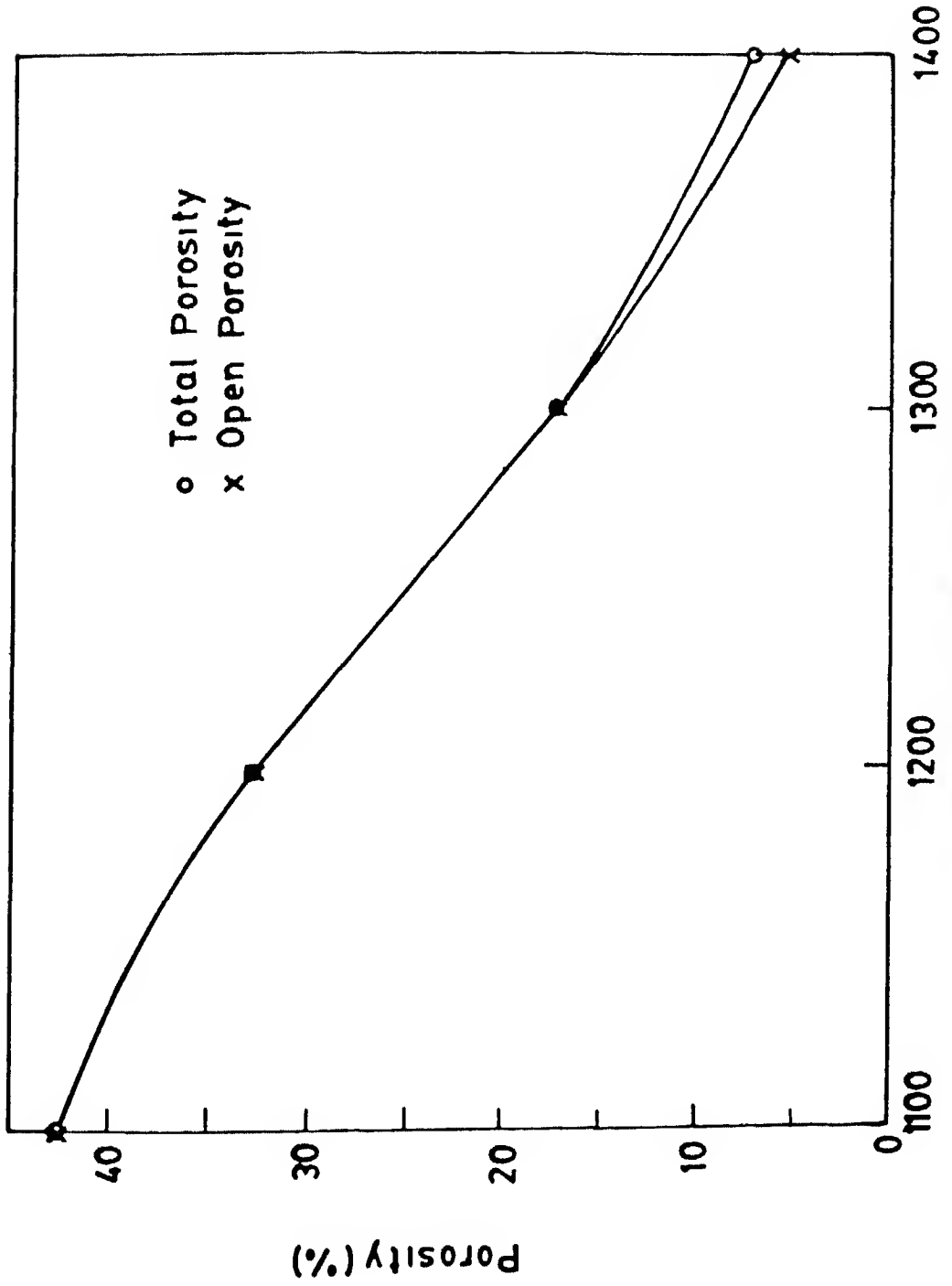

Fig 4 1 Variation of open and true porosity with sintering temperature for supports sintered for 1 hour

in porosity At the highest sintering temperature some pores begin to get isolated from the interconnected pore network due to pinching off of pore channels so that some closed porosity begins to appear

Our interest is having all the pores open This and a total porosity of 40 - 50/ as well as the requirement of sufficient mechanical strength led to our choosing pellets sintered at 1100 C/ 1 hr as the candidate material for supports for our membranes

4 1 2 Pore size and pore size distribution of the supports

With the help of mercury porosimeter the pore size and pores size distribution of the supports was determined

Fig 4 2 shows an intrusion - extrusion curve for the α-Al_2O_3 support The steep gradient of the intrusion curve at 0 8 μm shows that the pores are essentially of one radius The intrusion data summary is listed below

Total pore area	=	7 399 m^2 / gm
Median pore diameter	=	0 0818 μm
Bulk density	=	2 3205 g/cc

The value for the bulk density matches nicely with that derived from Archimedes method The very small pore size of the support itself ensures that the support is a very good micro porous membrane by itself with 42% of pores (all of which are open) and an average pore size of 0 08 μm

From the intrusion curve and eqn 3 6 the volume pore size distribution function D_v is plotted against the pore size of the support [Fig 4 3] It shows a peak at 0 08 μm corresponding to a unimodal pore size distribution All the pores are essentially of one size with a spread of 0 04 μm

The pore size and pore size distribution of the substrate material compare well with the available data Most workers procured high

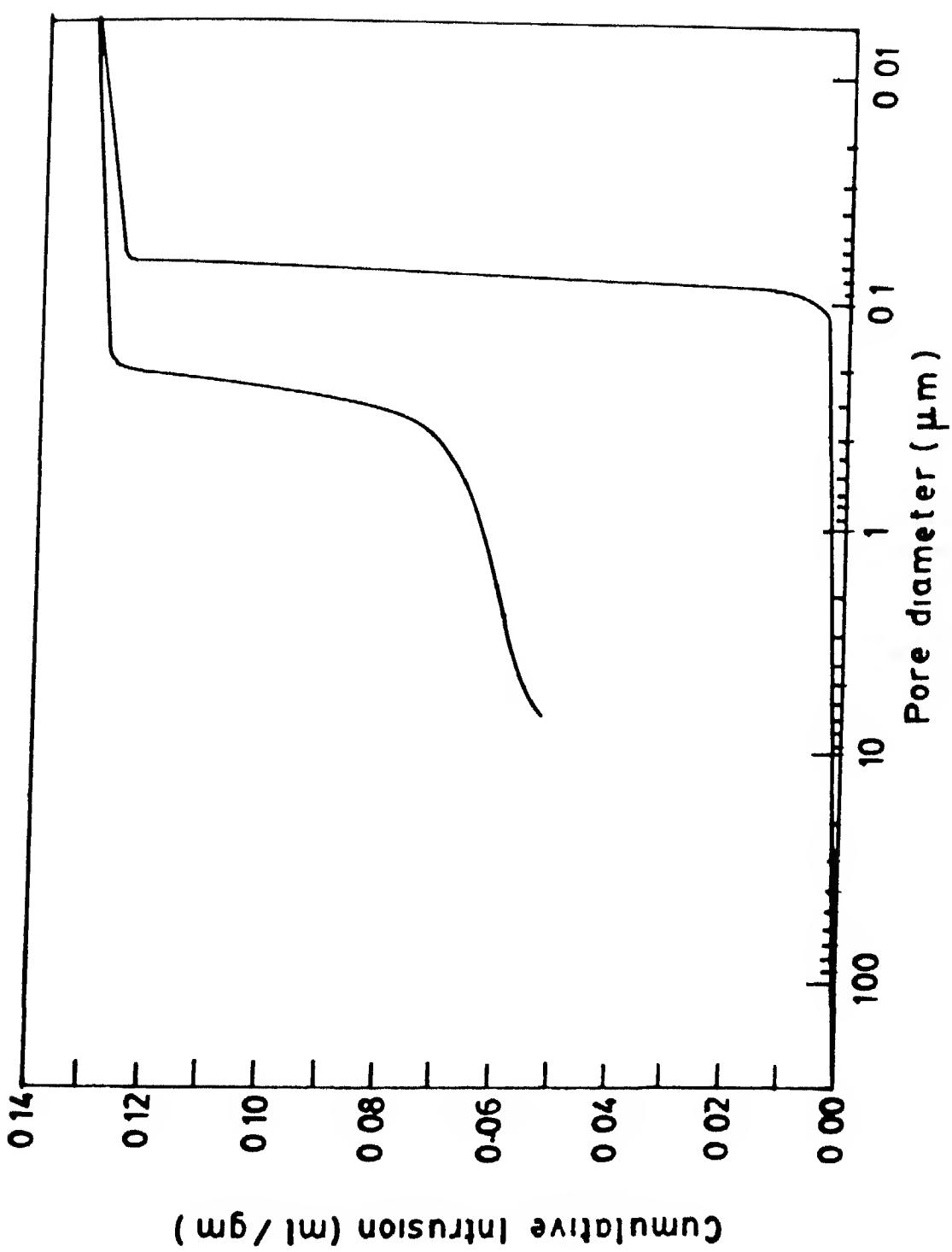

Fig 4 2 Mercury Intrusion - extrusion curve for the alumina support

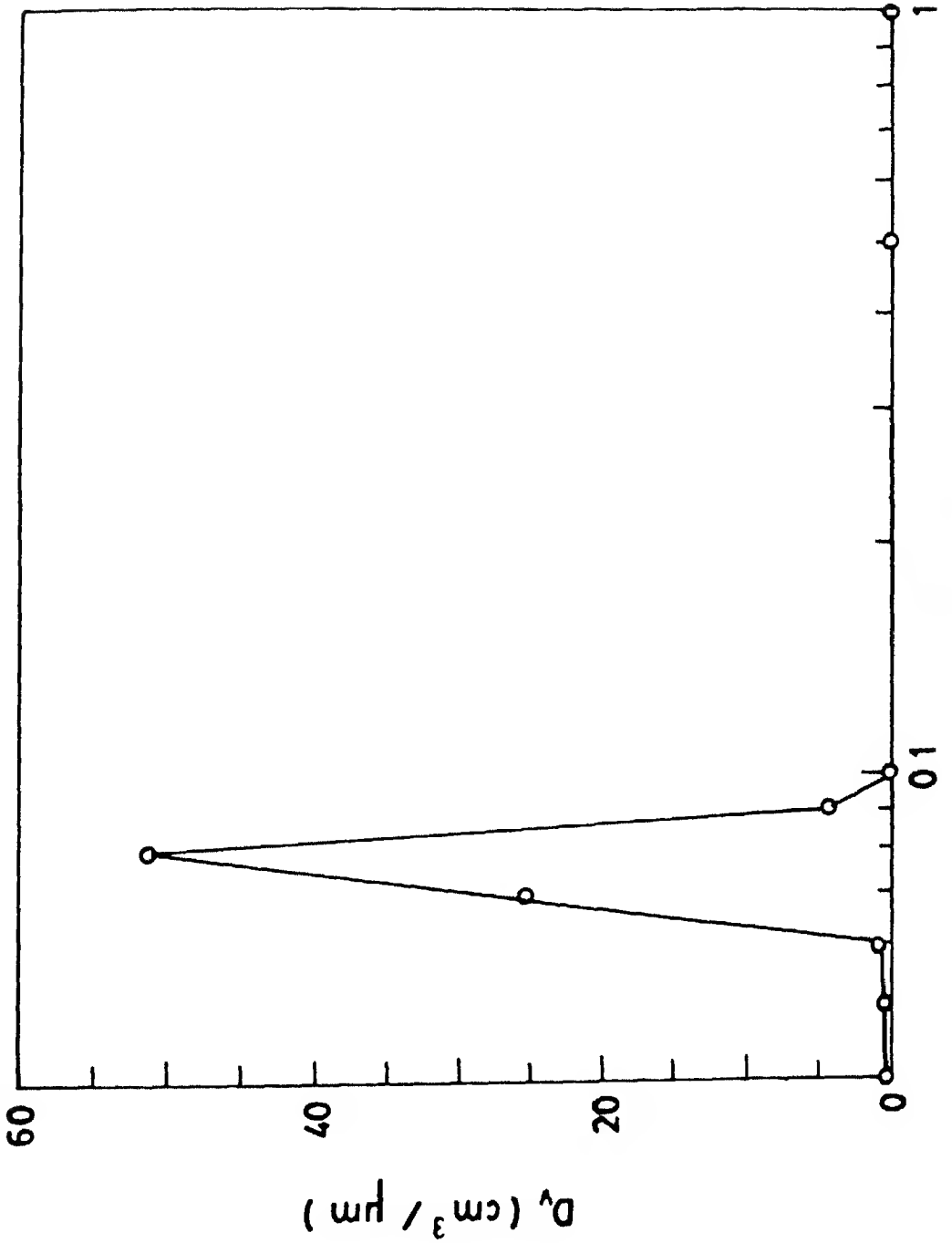

Fig 4 3 D_V vs Pore diameter for support

quality α - Al_2O_3 support disks from the market with known pore sizes and used them as membrane supports In our case we had synthesized the supports ourselves The type of supports used by different workers and the type that we used are compared in Table 4 2

Table 4 2 The different types of supports used by previous workers compared to the ones used in this study

Support material	Size	Avg pore radius (μm)	Pore size distribution	Ref
α-Al_2O_3	3 9cm ϕ x Ø 2 cm thick	Ø 12	Narrow	11
		Ø 34	Wide bimodal	11
		Ø 80	Wide bimodal	11
α-Al_2O_3	4 Øcm ϕ x Ø 2 cm thick	Ø 10	Narrow	23
α-Al_2O_3	3 9cm ϕ x Ø 2 cm thick	Ø Ø6	Narrow	24
α-Al_2O_3	2 54cm ϕ x Ø 3 cm thick	Ø Ø4	Narrow	This study

4 1 3 Fracture Strength Measurements

Fracture strength of small bars made out of the supports were measured using eqn 3 4

A total of eight samples were tested The fracture strength varied from 62 59 MPa to 91 99 MPa

Average fracture strength was 77 21 MPa For comparison it may be noted that the fracture strength of alumina bodies sintered at 1600°C (99% sintered density) is between 250 to 300 MPa

4 2 EFFECT OF DIPPING TIME ON MEMBRANE THICKNESS

The cross sectional view of the fractured surface of the membranes as seen in SEM gave an accurate estimate of the thickness of the γ-

Al_2O_3 layer Ideally the as deposited films should have been used to study the variation in film thickness with dipping time But according to Leenaars [11] the thickness of the calcined films are independent of the calcination temperatures hence the calcined films are good enough for the purpose

The variation of membrane thickness with square root of the dipping time in the sol is shown in Fig 4 4 The thickness of the membranes were determined from the fractured surface of SEM micro graphs [Fig 4 18 and Fig 4 19] by a method that has been described already The measurements were approximate due to local thickness variations From the figure it is seen that the membranes dipped for 10 seconds 20 seconds and 30 seconds in the sol gave results which can be fitted to a straight line with very high correlation thus proving that the slip casting mechanism is operating in this case The deviation observed in the plot for the 90 seconds membrane is quite substantial This could be due to an error in the measurement of thickness or there could be a real deviation from the slip casting mechanism This will need to be further studied

These results show that the dip - coating process of casting the membrane top layer on the porous support is essentially a slip - casting process at least in the early stage Due to the high capillary forces sol particles get sucked inside the pores of the support This results in pore constriction and ultimate pore blocking The increased concentration near the support surface leads to gelation of the adhered layer Subsequent calcination results in a homogeneous membrane layer

It must be remembered that the pore size of the support is an important parameter that determines the formation of the gel layer during dip coating in the sol If the sol concentration is too low and the pore size of support too large then gelation takes a longer time If the sol concentration is high and the support pore is too small then membrane layers tend to be thick and prone to cracking

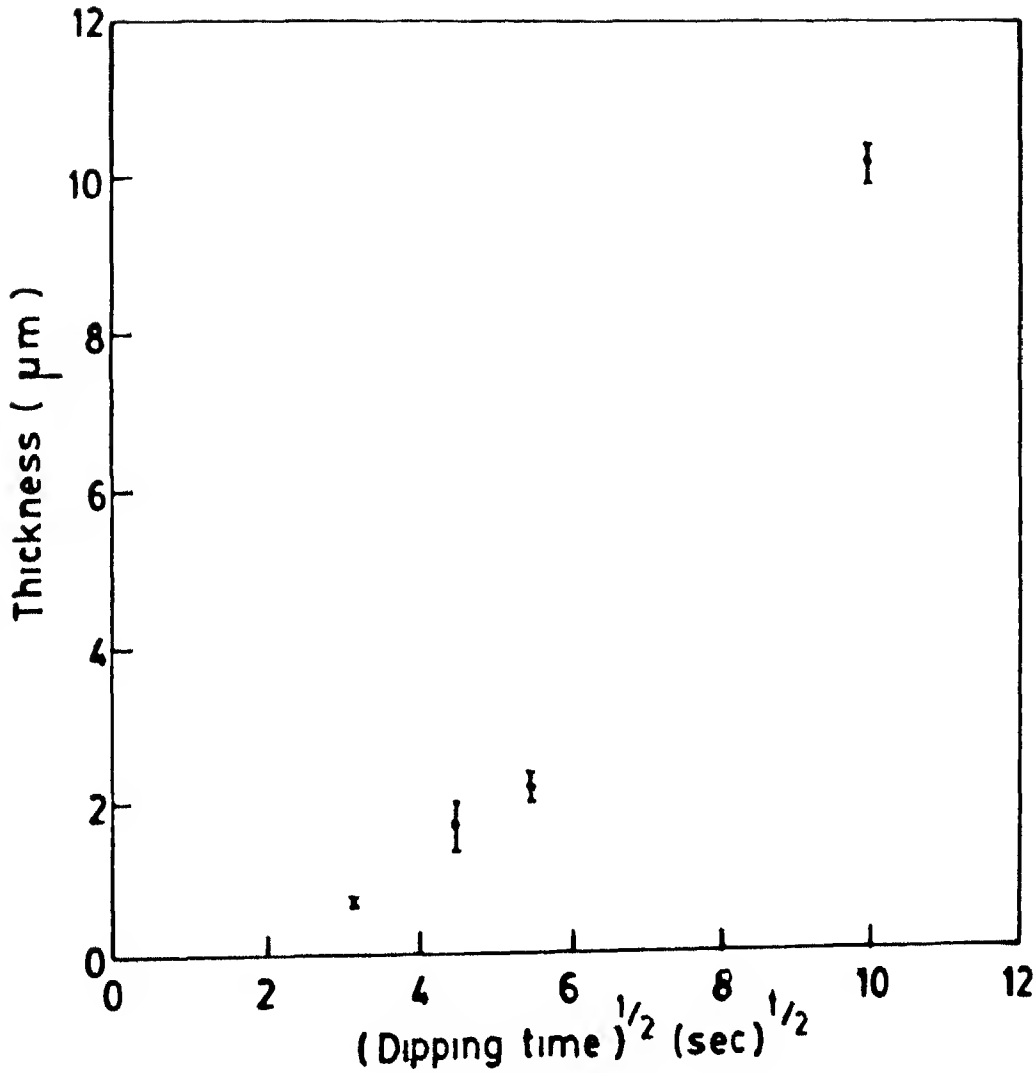

Fig 4 4 Variation of membrane thickness with dipping time in the sol

Since our supports had pore size in the lower pore size range we chose a very dilute sol concentration to obtain crack free thin top layers The sol concentration chosen by us was Ø 2 mol of boehmite/lt which compares with Ø 72 mol/lt chosen by Leenaars et al [11] for coating supports with average pore radius of Ø 34 μm

4 3 PHASE ANALYSIS

The X - ray diffraction patterns of gel - derived powders calcined at various temperatures is shown in Fig 4 5 The patterns corresponding to 300 C and 400 C are those of well crystallized boehmite At 500 C the calcined powder shows the peak corresponding to γ - Al_2O_3 There is a slight shift in the (400) peak which is at 2θ = 46 2 With increasing temperature the peaks corresponding to γ -Al_2O_3 get sharper which signifies its complete crystallisation The powders calcined at 700 C and higher temperatures show an increase in the intensity of the (440) peak This shows the presence of a mixture of both the γ and δ phases The patterns for 900 C and 1000 C show a particularly large crystallite size

The phases detected in calcined membranes by Leenaars et al [10] compared with our data is shown below

Table 4 3 Comparison of the Phases detected in calcined gels

Temperature (C)	Phase (Leenaars)	Phase (This study)
200	γ - AlOOH	—
300	—	γ - AlOOH
400	γ/δ - Al_2O_3	γ - AlOOH
500	γ/δ - Al_2O_3	γ - Al_2O_3
600	γ/δ - Al_2O_3	γ - Al_2O_3
700	γ/δ - Al_2O_3	γ/δ - Al_2O_3
800	γ/δ - Al_2O_3	γ/δ - Al_2O_3
900	θ - Al_2O_3	γ/δ - Al_2O_3
1000	α - Al_2O_3	γ/δ - Al_2O_3

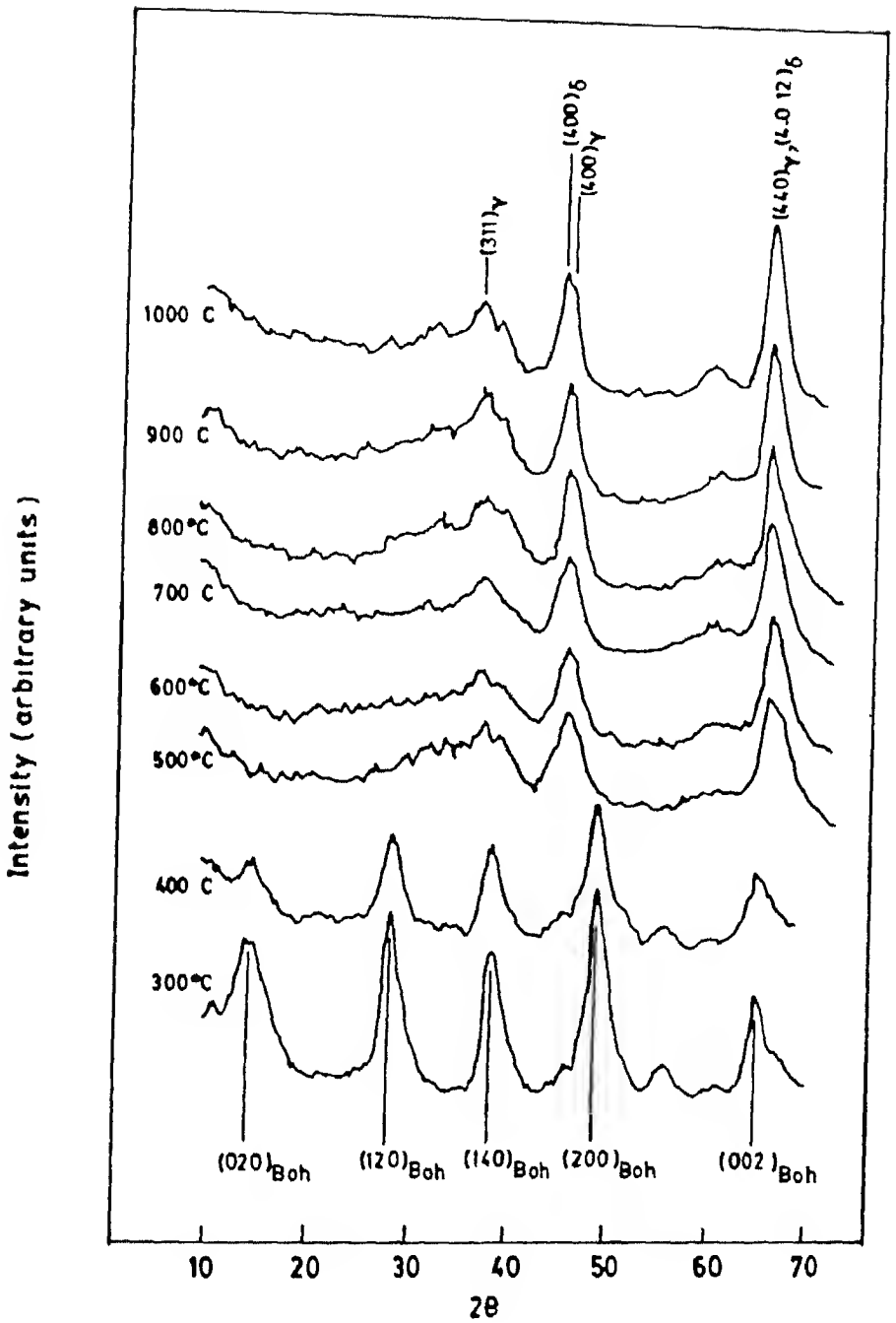

Fig 4 5 X - Ray diffractograms of gel-derived powders calcined at various temperatures

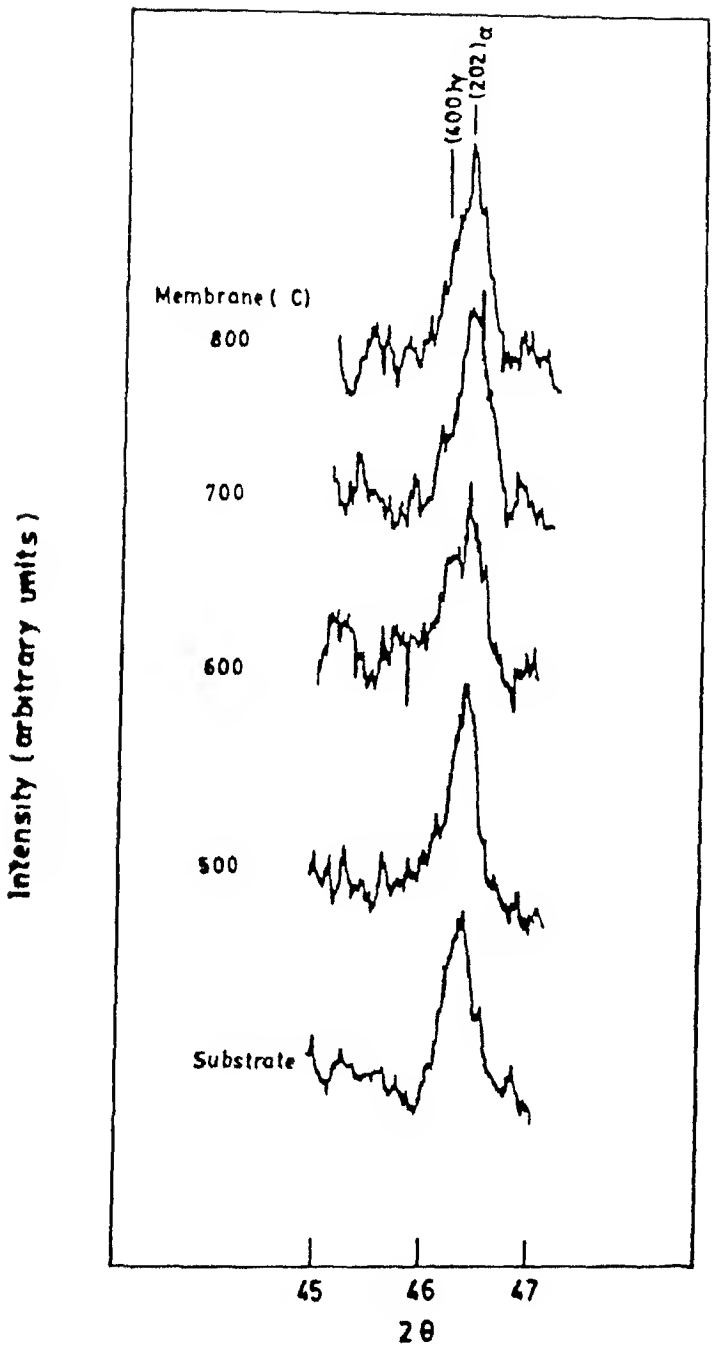

Fig 4 6 X - Ray diffractograms of the support and the supported membranes calcined at various temperatures

The X - ray patterns of the membranes on the α - Al_2O_3 supports were taken It is shown in Fig 4 6 The peaks of the substrate overlap with that of the membrane, which is γ - Al_2O_3 However after comparing the pattern obtained from the substrate with that from the membrane it can be definitely said that there is a broad peak corresponding to γ - Al_2O_3 at 46 (2θ)

4 4 THERMAL ANALYSIS

The TG plot of the powder sample dried at 80 C and heated at 10 C/ min is shown in Fig 4 7 There is a gradual weight loss till 450 C corresponding to the slow removal of organic and molecular water Maximum weight loss is about 50% After 500 C a constant weight is reached

DTA plot in shown in Fig 4 8 The endothermic peak at about 80 C correspond to the removal of alcohol A small exothermic peak at 224 C signifies removal of organics followed by an exothermic organic burn out peak at 255 C The crystallization onset is signified by the broad exothermic peak at about 516 C The exothermic peak at 1100 C correspond to the sintering process

4 5 INFRARED SPECTRA

The infra - red spectra of the gel derived powders are shown in Fig 4 9 As can be seen in the as dried powder the broad OH^-band (3000 -3700 cm^{-1}) corresponds to intercalated water and /or alcohol groups The 1600 - 1700 cm^{-1} band corresponds to a stretching of C = C bonds it can also be an overtone of the OH^- band The 1300 - 1500 cm^{-1} band corresponds to the C -H bond (bend in plane) The sharp peak at 1400 cm^{-1} is probably due to the butyl group which is attached to the Al atom This peaks gets reduced in intensity with increasing temperature probabaly due to the removal of the butyl group as butanol At 600°C the only peaks are those of C = C and the OH The residual OH groups at 600 C probably lead to poor crystallization observed at that temperature

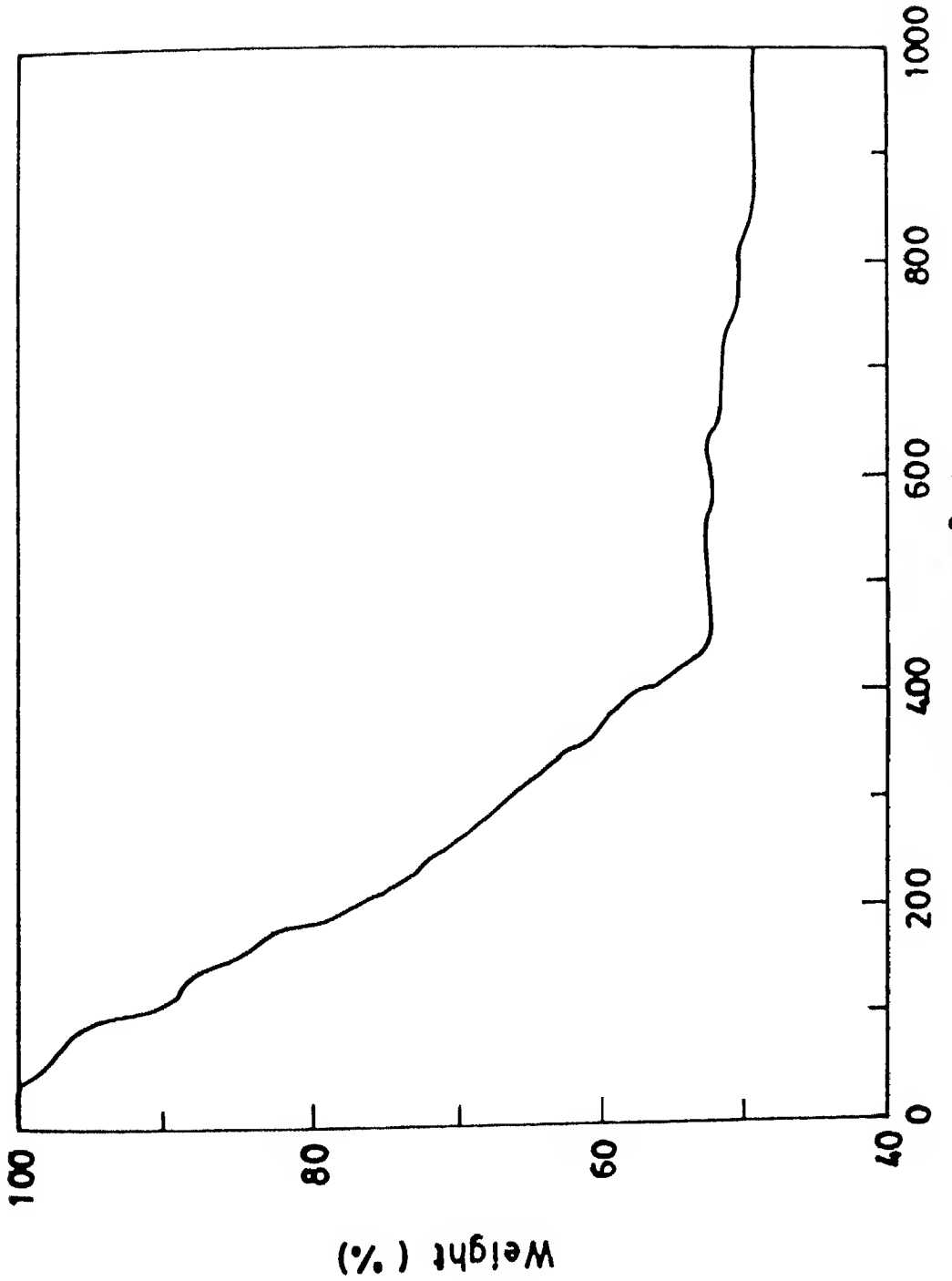

Fig 4 7 Thermogravimetric plot of the gel derived powder at 10°C/min

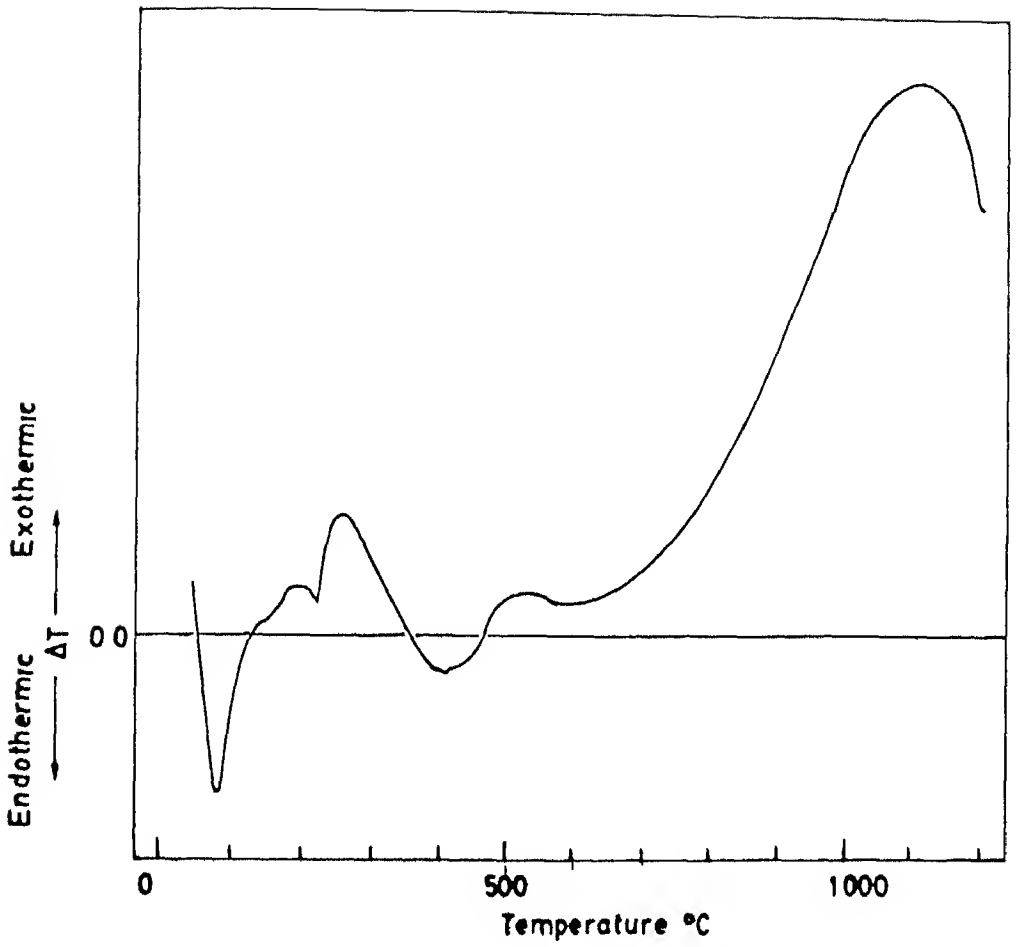

Fig 4.8 DTA plot of the gel derived powder at 10°C/min

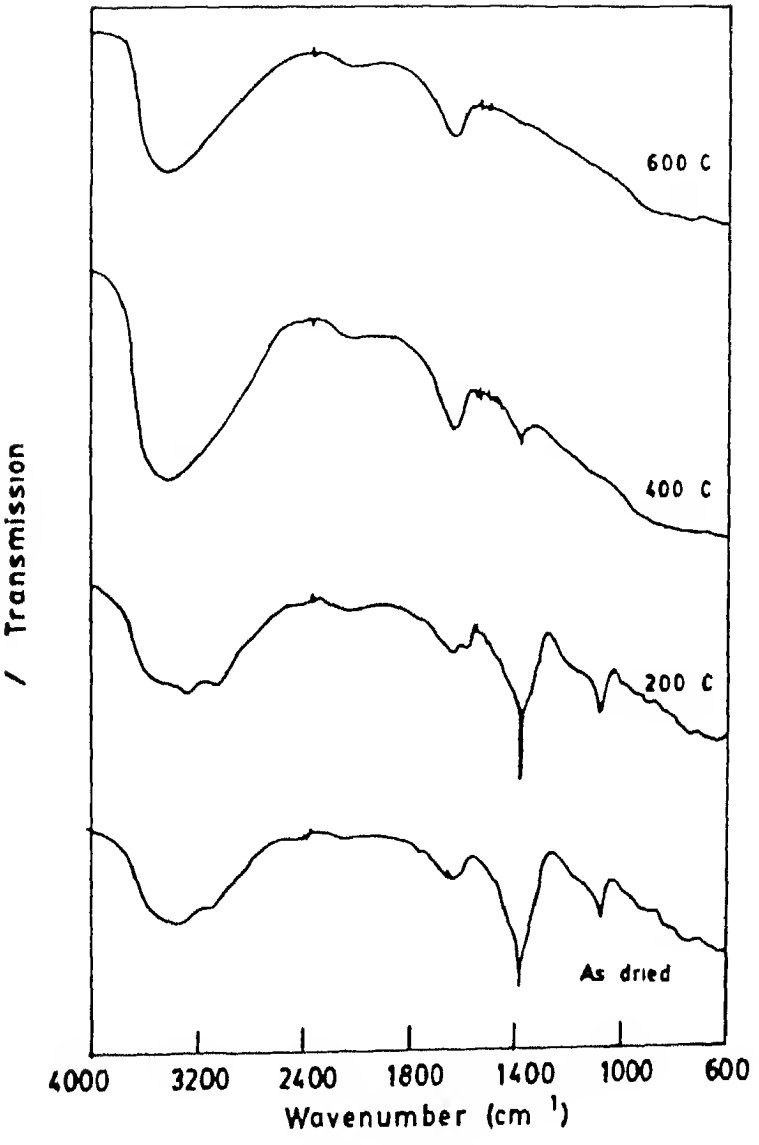

ig 4 9 Infrared spectra of the gel derived powders as a functio of temperature treatment

4 6 NITROGEN ADSORPTION - DESORPTION STUDIES

The specific surface areas and pore sizes of supported membranes calcined at 500 C 600 C 700 C and 800 C for 3 hours were measured using the shown in Table 4 2

Table 4 4 Specific surface area and average pore diameter of supported g-Al_2O_3 membranes calcined at different temperature for 3 hrs

Temperature of calcination (C)	Specific surface area m^2/gm	Average pore pore diameter (nm)	Porosity %
500	273	3 9	49 3
600	253	4 2	49 2
700	174	6 1	49 2
800	152	7 2	49 9

The specific surface areas and average pore diameters were calculated using eqn 3 8 and 3 9 respectively and the porosity was calculated for the membranes assuming cylindrical pore geometry and assuming that the adsorption takes place on the curved surface of the pores [Annexure I]

Fig 4 10 and 4 11 show the variation of specific surface area and the average pore diameter of the supported membranes with the calcination temperature

It is seen from Table 4 2 that the specific surface area decreases while the average pore diameter increases with increase in the calcination temperature Fig 4 10 and 4 11 show that the variations are complementary to each other The porosities of the membranes however remain the same This can be explained by the fact that with increasing temperature smaller pore density decreases and lager pore density increases This can happen if smaller size pores coalesce to form larger sized pores at higher

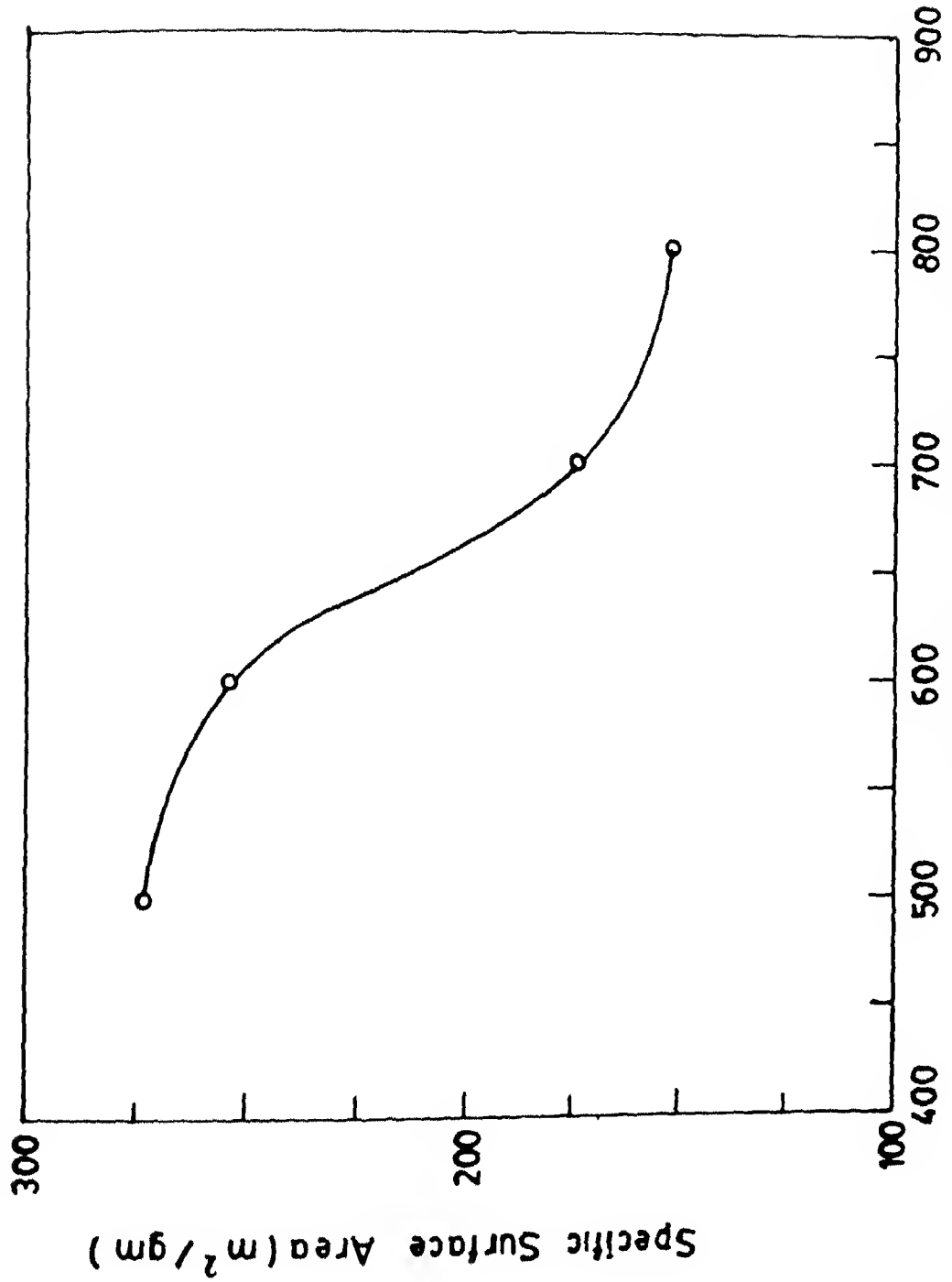

Fig. 4.10 Variation of specific surface area with calcination temperature for supported membranes

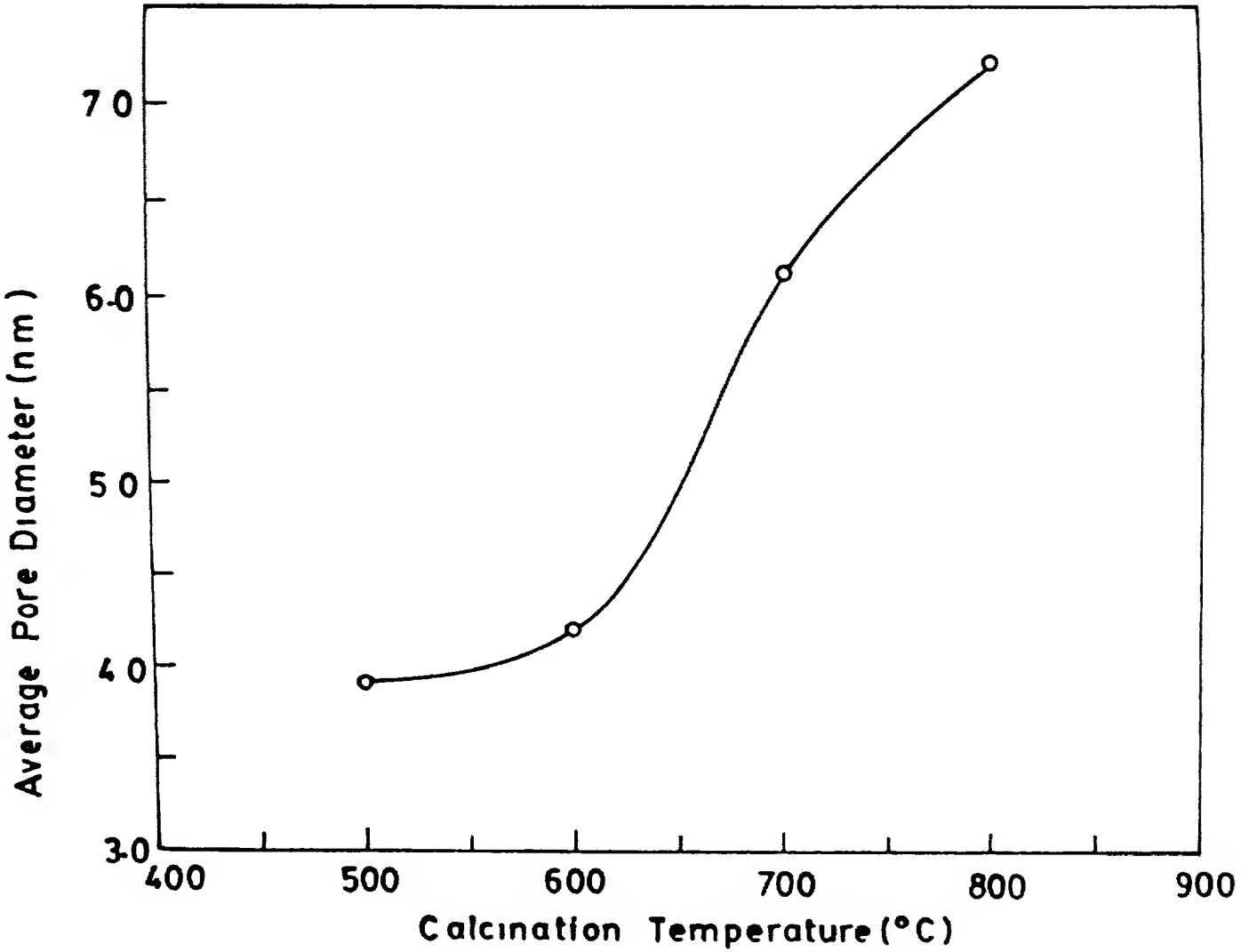

Fig 4 11 Variation of the Average Pore Diameter with calcination temperature for supported membranes

temperatures The nature of the plot in Fig 4 10 show that the specific surface area shows a nominal decrease between 500 C and 600 C decreases sharply thereafter and then flattens out This corresponds to a coarsening of the microstructure Crystallization of γ - Al_2O_3 continues between 500 C and 600 C however after 600 C, when crystallization is over grain growth starts resulting in large grains which is also shown by the albeit slight narrowing of the X - ray peaks [Fig 4 5] The pore size variation shows a similar nature in the complementary sense which can also be explained by similar reasoning

4 7 WATER PERMEABILITY TESTS

Table 4 3 shows the results for water permeability tests done on membranes calcined at 500 C, 600 C 700 C and 800 C in an UF cell in the dead end permeation mode The details of the experimental procedures have already been provided [Sec 3 3 9]

Table 4 5 Water Permeability Results on membranes calcined at different temperatures for 3 hours

Pressure (Psi)	Water flux (cm/s) x 10^{-4}			
	500°C membrane	600 C membrane	700 C membrane	800 C membrane
0	0	0	0	0
100	5 93	7 36	12 17	17 24
150	8 47	9 32	17 35	26 69
200	10 69	11 89	23 18	35 29
250	13 03	13 98	26 74	39 54

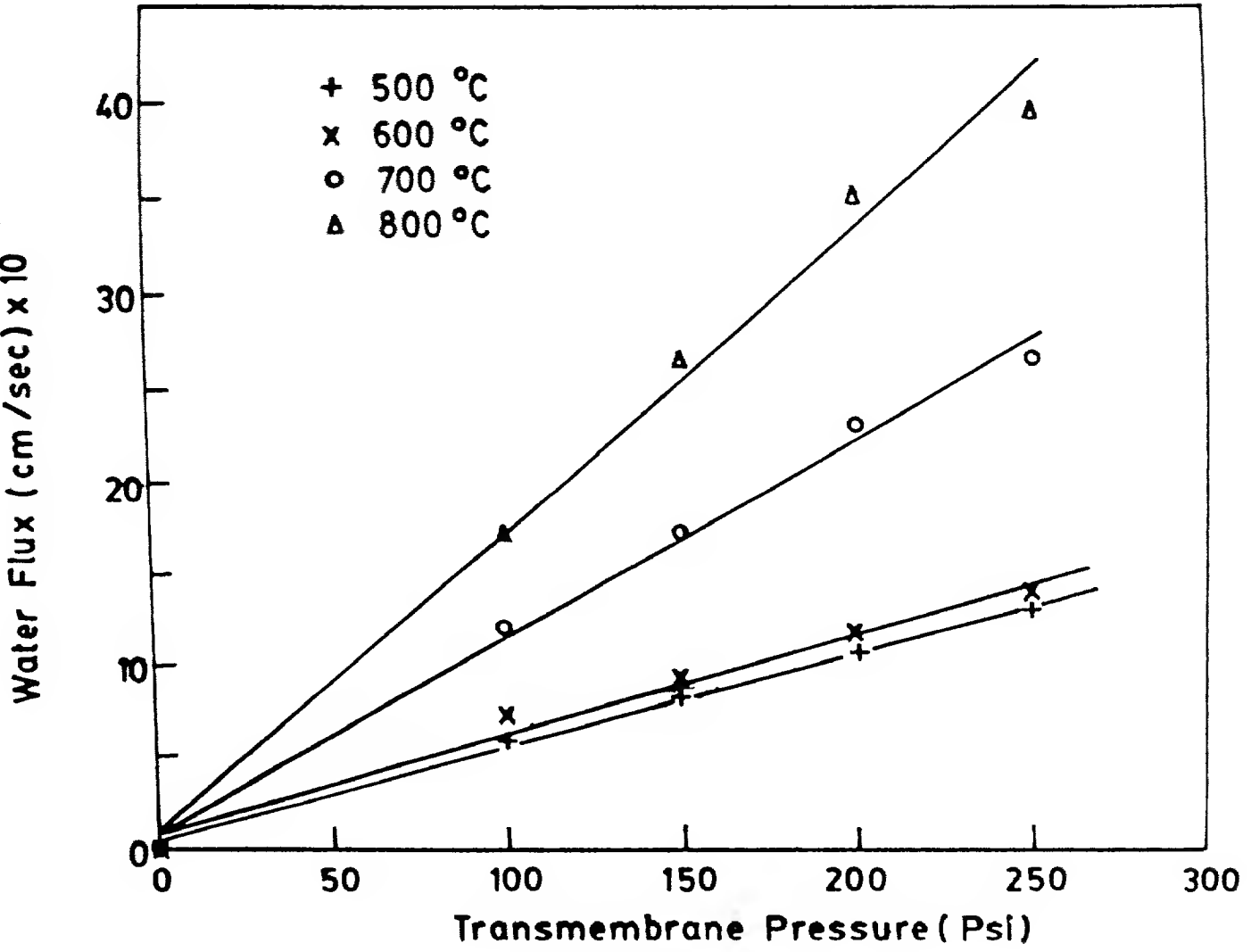

Fig 4 12 Variation of water flux with the applied pressure for membranes calcined at different temperatures for 3 hours

The variation of water flux with operating pressure is governed by Darcy s Law

$$J_w = L_p \Delta P = \frac{\Delta P}{R_m \eta} \qquad (4\ 1)$$

Where R_m = membrane resistance

L_p = membrane permeability

η = viscosity of water

J_w = water flux and

ΔP = applied pressure

The permeability is a measure of the pore size of the membrane For higher pore sizes the permeability is greater

The variation of the water flux with pressure was indeed found to be linear conforming the above eqn and shown in Fig 4 12 The membrane permeabilities were obtained from the plot of water flux vs ΔP plots

The permeability was found to increase with the calcination temperature of the membrane There is no appreciable change in the permeability at low calcination [0 0519 cm/s - psi X 10^{-4} for 500 C membrane and 0 0554 X 10^{-4} cm / s- psi for 600 C membrane] But the permeability increases rapidly thereafter being 0 1086 X 10^{-4} cm / s - psi for 700 C membrane and 0 16335 X 10^{-4} cm / s - psi for 800 C membrane Thus there is a threefold increase in the permeability with increase in calcination temperature 500 C to 800°C

The internal surface area/unit volume of the membrane material, S, is related to the membrane resistance R_m by the following relation obtained by comparing Eqn 4 1 and Eqn 3 11

$$\frac{\varepsilon^3}{\eta\ K\ (1-\varepsilon)^2\ S^2\ L} = \frac{1}{\eta\ R_m} \qquad (4\ 2)$$

Here ε = porosity of membrane

η = Viscosity of the liquid (gm/cm-s)

K = Kozney Carman constant

S = Surface area/unit volume of membrane material (cm^2/cm^3)

L = Thickness of the membrane layer (cm)

R_m = Membrane resistance

Eqn 4 2 suggests that S^2 varies linearly with ηR_m provided K ε, L are constant which is true in this case Figure 4 13 plots S_m^2 against ηR_m for the four different membranes S_m^2 values are those obtained from BET and directly correspond to S^2 values since the material is the same for the four membranes and the porosity is constant ηR_m values are taken from the water permeability results The plot shows a linear dependence of S_m^2 on ηR_m and the correlation coefficient of the best fitted straight line was found to be Ø 993 This shows that the results from BET tests and water flux measurements agree well, and the pore diameters predicted by both these methods match closely

4 8 PEG Permeation and Retention Tests

The flux decline behaviour was studied using PEG 4000 in an unstirred mode ultrafiltration system with membranes calcined at 500 C 600 C, 700 C and 800°C for 3 hours The experimental details have already been explained [3 3 10]

The variation of flux (J) was plotted against the time elapsed from the start of the experiment It is shown in Figure 4 14 The flux decline behaviour predicted from Eqn 3 13 is indeed observed

The flux decrease is fairly rapid for the membranes calcined at 800°C and 700°C (membranes with larger pore size) For 800 C membrane it drops from 1 Ø5 x 10^{-9}cm/s after 2 minutes to Ø 28 x 10^{-9}cm/s after 138 minutes It means a drop of nearly 73 % of the initial value For the 700 C membrane it shows a similar drop from Ø 939 x 10^{-9}cm/s (after 3 minutes) to Ø 264 x 10^{-9}cm/s (after 90 minutes) But for membranes calcined at 500 C and

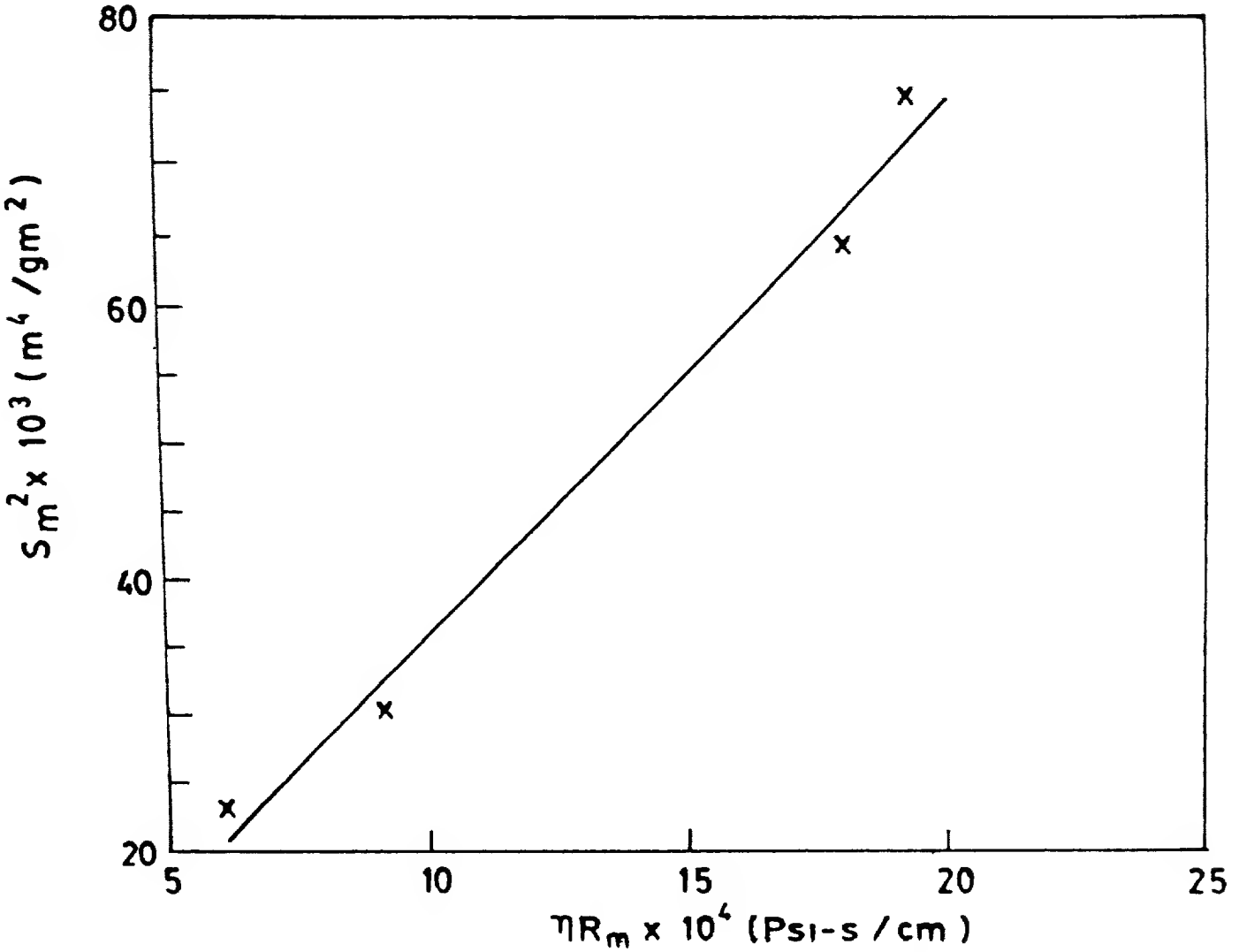

Fig 4 13 S_m^2 vs ηR_m

60Ø C the decline is less spectacular (about 6Ø % for both) The initial flux for these membranes are also very low about Ø 57 to Ø 58 x $1Ø^{-5}$ cm/s

The results can be understood by considering the phenomenon of concentration polarization due to osmotic pressure build up near the membrane solution interface Flux decline is not due to gel layer formation since the solute chosen PEG 4ØØØ has a quite a low molecular weight and high gel concentration which can never be reached in practice [4Ø] The osmotic pressure limited flux of solute is understood by Eqn 3 13 With the elapse of time the concentration of rejected solutes increase the membrane surface concentration C_m and increases the osmotic pressure π of the solute near the membrane surface This results in the reduction of the driving force causing a decline of flux A constant downward trend is observed in the flux decline behaviour because the process is basically an unsteady state one and a constant constant flux value is never reached

The faster rate flux decline for membranes with larger pore size can be explained as follows When pore size increases R_m decreases, consequently the permeability of the solvent through the pore increases This result in a faster rate of transport through the pores which also cause a rapid increase of the concentration of the rejected solute near the membrane surface Since osmotic pressure is associated with this increase in C_m the rapid increase in osmotic pressure cause a rapid decline in the driving force and consequently the flux Though the solute rejection is high for smaller pore sized membranes, due to high R_m, flux is quite low and the decrease is less dramatic

The flux decline behaviour as predicted by Chudacek and Fane [38], Wijmans [39] and Daves [4Ø] was put to test for these membranes In a manner similar to theirs a plot of $1/J^2$ Vs time was made A best fit linear plot confirmed their theory of unstirred batch ultrafiltration Whereas they proved the theory for higher molecular weight solutes, our present data match

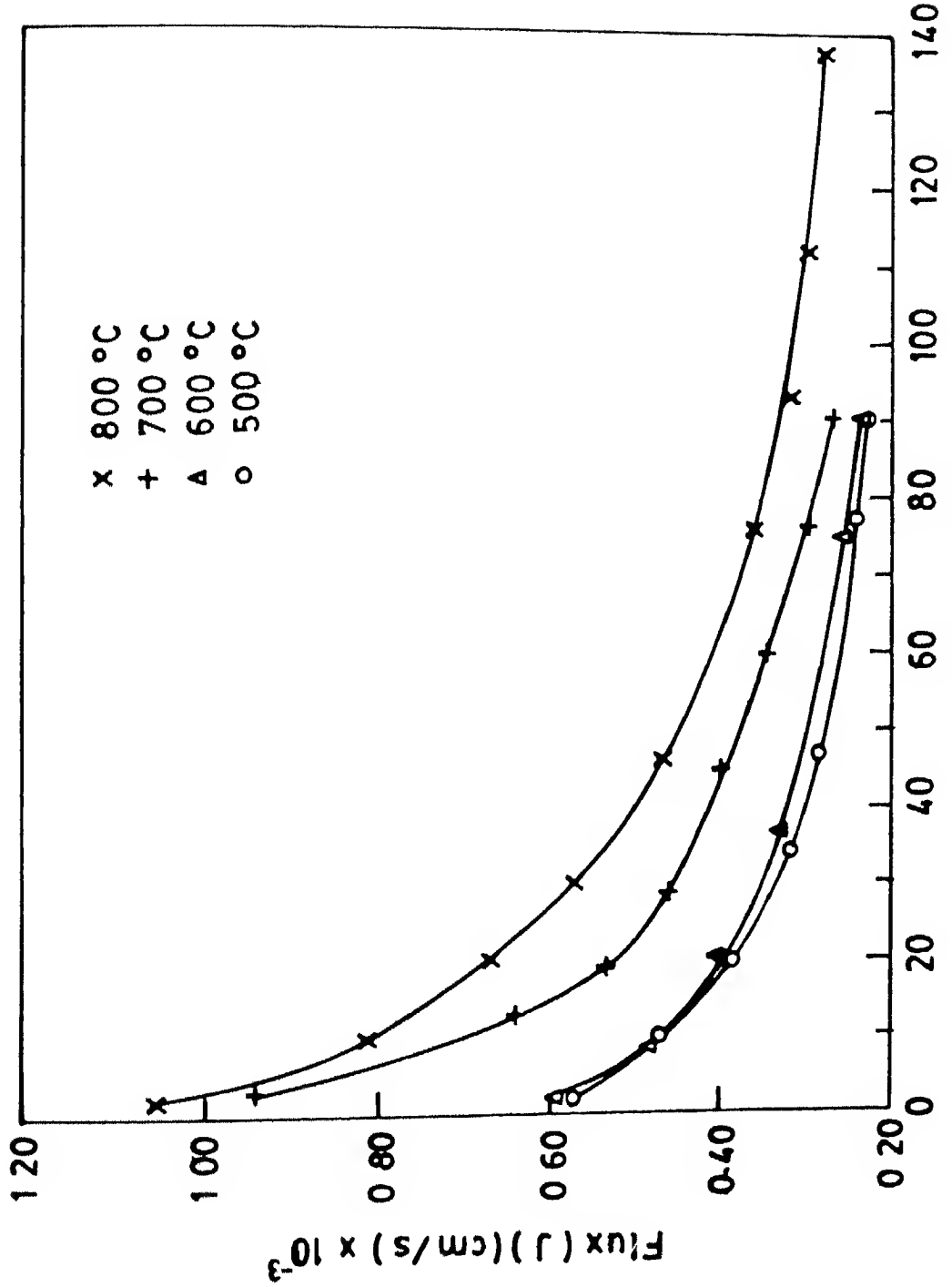

Fig. 4.14 Flux declined behaviour with PEG 4000 observed for membranes calcined at different temperatures for 3 hours

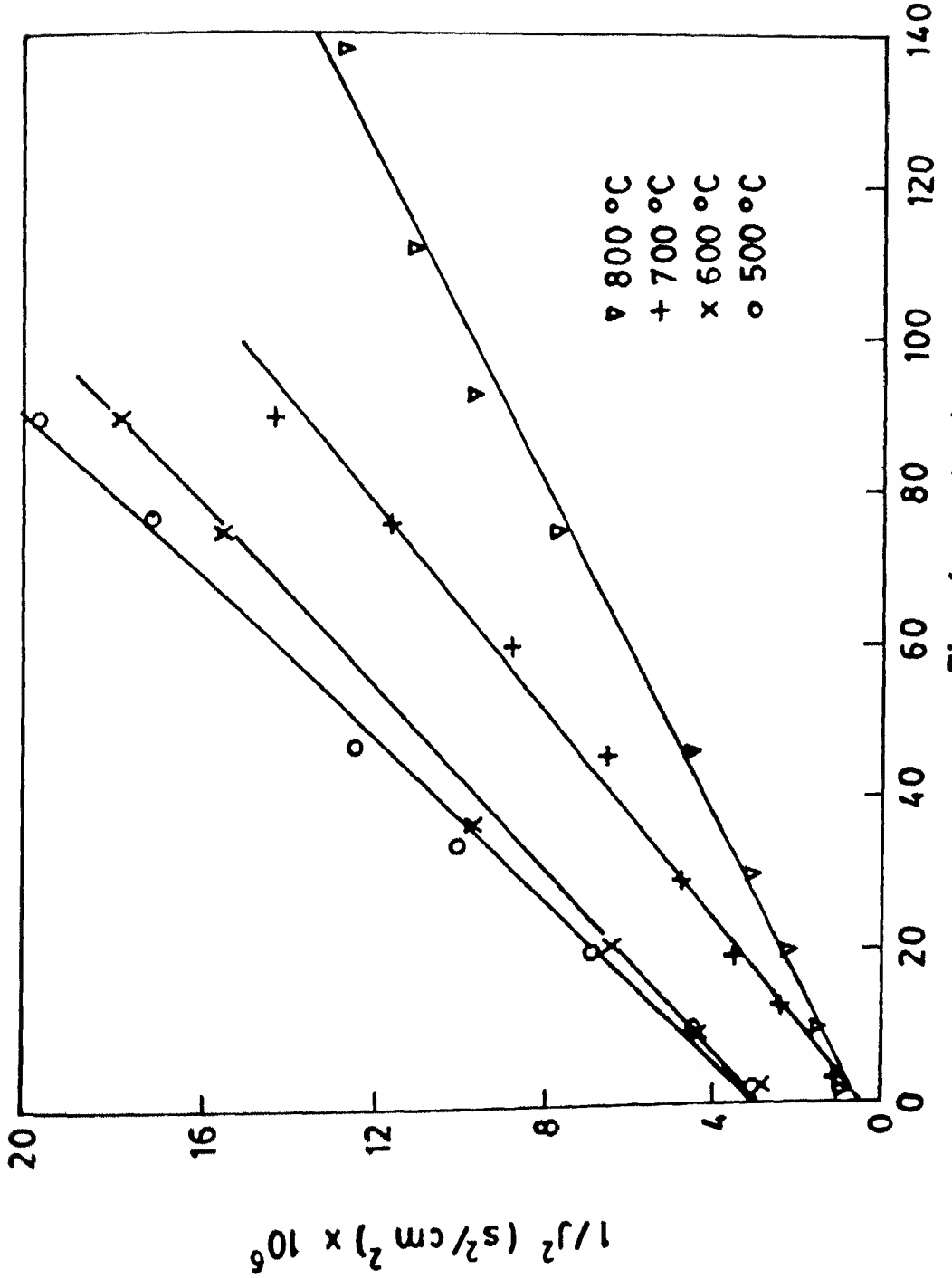

Fig 4.15 Plot of $1 / J^2$ vs. time for PEG 4000

the same for lower molecular weight solutes as well The relevent plot is shown in Fig 4 15 All the lines of best fit had a correlation coefficient of Ø 99

The y-intercept (c) of the line is related to the effective resistance by $R_m = \Delta P \times \sqrt{c}$

From this relation the values for R_m obtained was 2 62 x 10^5 g/cm^2-s for 5ØØ C membrane and 1 125 x 10^5 g/cm^2-s for 8ØØ c membrane These are much higher than that obtained from water run (2 x 10^5 g/cm^2-s for 5ØØ C and Ø 625 x 10^5 g/cm-s for 8ØØ C) The difference may account for the polarization resistance for these two membranes

The solute rejection characteristics of these membranes were also measured using PEG 4ØØØ and 6ØØØ The results obtained are given in Table 4 6

Table 4 6 The observed PEG rejection of the membranes calcined at different temperatures

Temp (C)	Pore diameter (nm)	Observed Rejection	
		PEG 4ØØØ	PEG 6ØØØ
5ØØ	3 9	4Ø 16	52 53
6ØØ	4 2	31 97	44 2Ø
7ØØ	6 1	23 77	35 86
8ØØ	7 2	15 57	27 54

A plot of the observed solute rejection against pore diameter was made [Fig 4 17]

The general trend of decreasing solute rejection with increasing pore size for a particular solute was seen The rejection of PEG 6ØØØ for a particular membrane was higher than that of PEG 4ØØØ for the same membrane This can be explained by the increase in the size of PEG with its

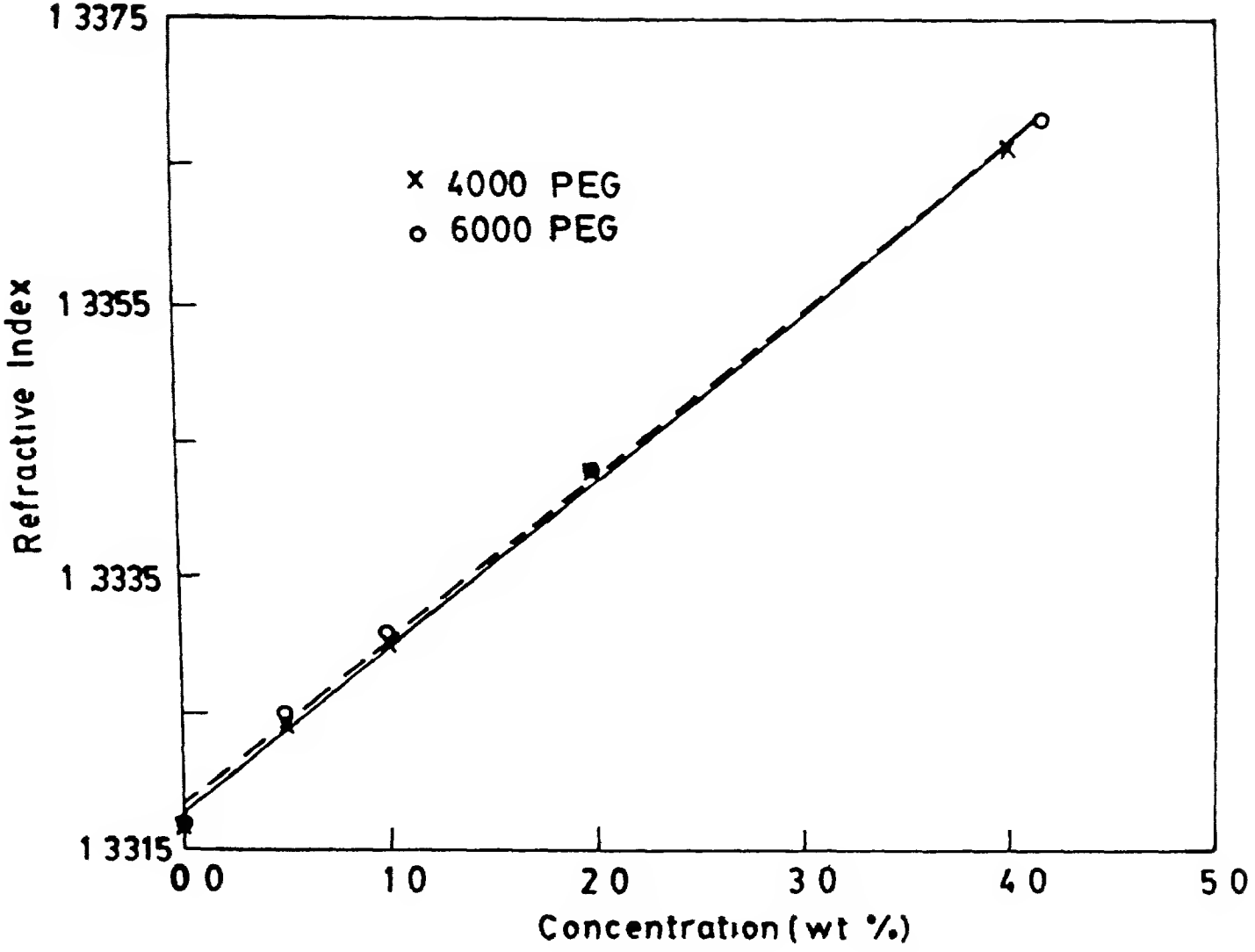

Fig. 4 16 Calibration Curve for PEG 4000 and PEG 6000

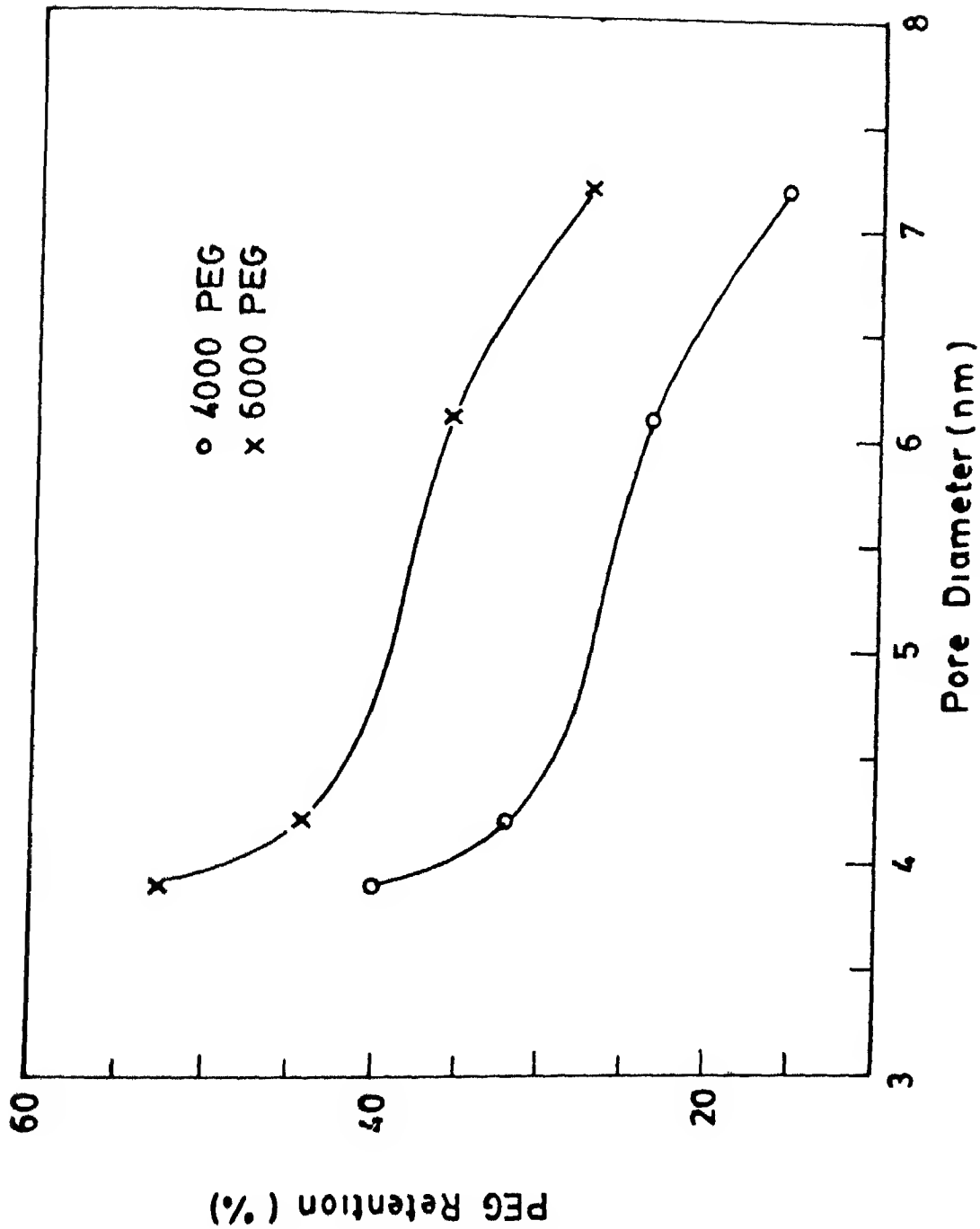

Fig 4 17 Observed solute rejection of PEG vs Pore diameter of membranes

molecular weight The rejection of the same PEG through a smaller pore is thus naturally higher

The PEG retention results show that they are quite low as compared to the data of Leenaars [13] He obtained a value of 87 % for a similar pore sized membrane with PEG 6000 This discrepancy can be explained by considering the following

The data presented here is for an unstirred cell Here solute rejection causes an increase in the solute concentration close to the membrane surface In ultrafiltration this can attain a value of 12-16 times the feed concentration depending on the osmotic pressure behaviour of the solute [14] The real rejection (R_r) defined as

$$R_r = (1 - C_p / C_m)$$

Where C_p = Permeate concentration

and C_m = membrane boundary layer concentration

will then be quite high For the data presented here R_r will be close to 96 % For unstirred cell data as presented by Leenaars stirring causes C_m to decrease to a value close to C_f so that real rejection is approximately equal to the observed

The above reason coupled with much higher operating pressure of 150 Psi has probably resulted in much lower flux observed

4 9 SCANNING ELECTRON MICROSCOPY

Figure 4 18 and 4 19 show the crossectional view of the membrane top layer dipcoated for 10 seconds and 30 seconds respectively as seen on the fractured surface of the support The micrographs show a 1-2 μm thick γ - Al_2O_3 layer on the porous α - Al_2O_3 support The grain size of γ - Al_2O_3 is very fine and could not be resolved properly This micrographs were

used for membrane thickness calculations Figure 4 20 shows the top surface of an unsupported γ - Al_2O_3 membrane calcined at 600°C The micrograph shows largeagglomerated grains loosely packed with more or less homogeneous and intercon-nected pores This kind of highly tortuous porosity is a typical feature of a γ - Al_2O_3 membrane

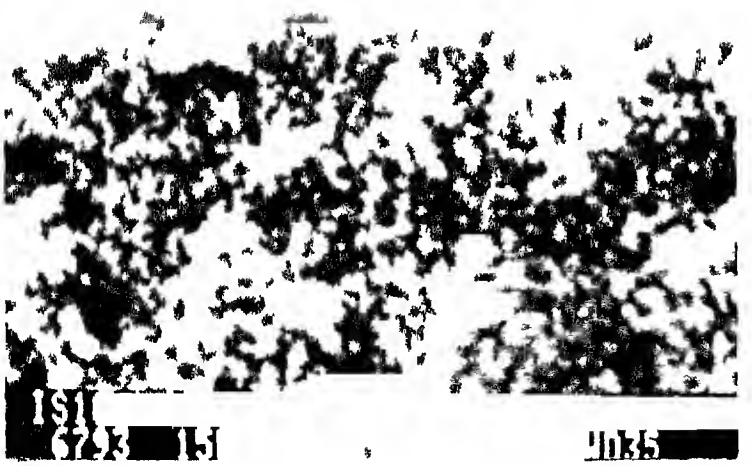

. 4 18 SEM Micrograph of a supported membrane dip coated fo
10 seconds and calcined at 600°C for 3 hours

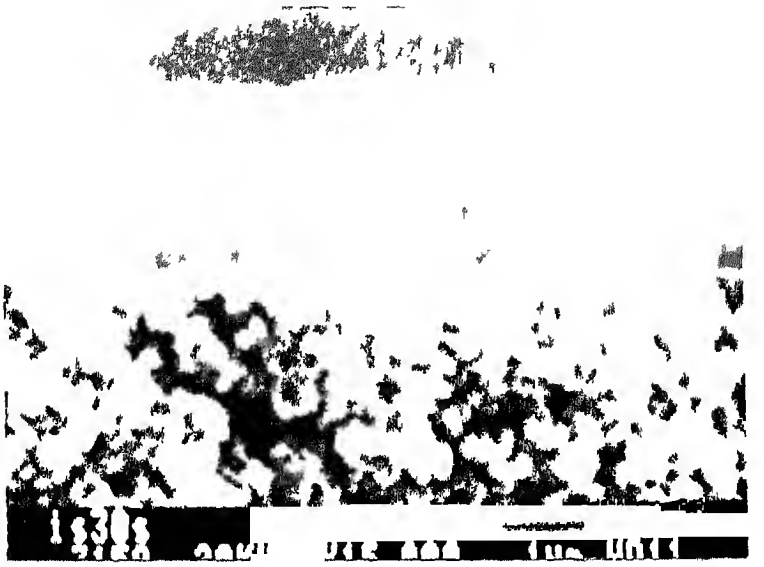

ıg 4.19 SEM Micrograph of a supported membrane dip coated for 30 seconds and calcined at 600°C for 3 hours

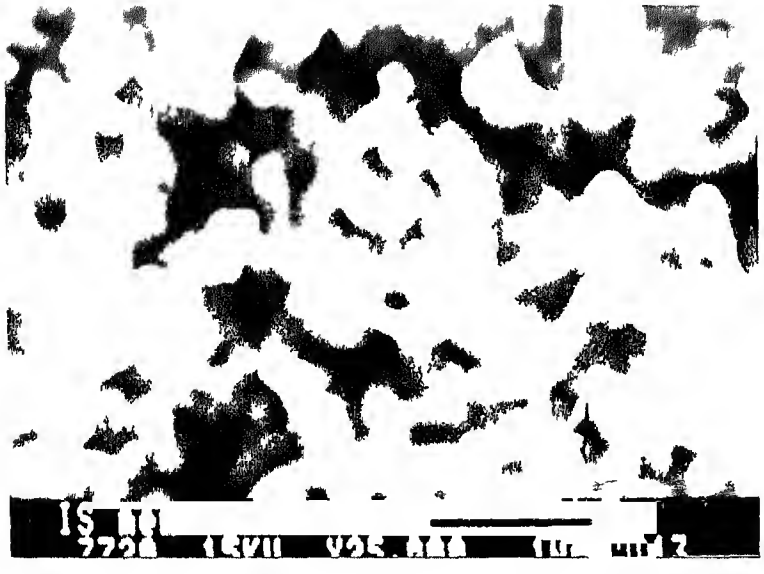

I 20 SEM Micrograph of an unsupported membrane calcined at 600°C/3 hours showing the membrane ultrastructure

5 CONCLUSIONS

1 This study entails the preparation and characterisation of supported γ-Al_2O_3 membranes which were synthesized by sol-gel route The membranes were crack free and thermally stable

2 The supports prepared from submicron α -alumina powder (Ø 3 μm) by conventional ceramic process route had a pore diameter of Ø Ø8 μm the lowest reported so far and a very narrow pore size distribution

3 The membranes were deposited from the peptised boehmite sols prepared by Yoldas method having alkoxide water ratio of 1 15Ø Much lower sol concentration (Ø 2 moles of boehmite /lt) could be used for membrane deposition than reported earlier

4 Dip coating technique was employed to slip cast the sol on the supports by varying the dipping time Much thinner and crack free membranes (about 1 to 2 μm) were obtained The thickness of the supported layer was found to be proportional to the square root of the dipping time there by confirming slip casting to be the deposition mechanism

5 The porosity, average pore diameter and specific surface area of the membranes were found to vary with calcination temperature Although the pore size increased and specific surface area decreased with increasing calcination temperature porosity remained the same

6 XRD studies on the calcined powders confirmed the presence of γ -AlOOH at low temperatures (below 4ØØ C) which subsequently changed to γ-Al_2O_3 on further heating At still higher temperatures (8ØØ C to 1ØØØ C) mixture of γ and δ phases were detected γ-Al_2O_3 was found to be present in the top layer of the supported membrane as well

7 A dead end permeation cell was used to study the water permeation characteristics of the membranes as a function of calcination temperature (500 C to 800 C) It was observed that the permeability increased with increasing calcination temperature thus validating the Kozney Carman equation for liquid permeability The membrane resistance (R_m) obtained from the water permeability data and surface area / unit mass (S_m) from BET were found to be in excellent agreement when used in the fluid flow equation

8 PEG flux decline behaviour of the membranes followed the unsteady flow equation Flux decline was higher for membranes of larger pore size This characteristic obtained for the first time proved that concentration polarization mechanism was applicable for ceramic membranes as well

9 Low values of solute rejection were observed for membranes tested with PEG 4000 and PEG 6000 This is attributed to the concentration polarization mechanism operating in unsteady state permeation

SUGGESTIONS FOR FURTHER WORK

1 Al_2O_3 membranes prepared by the sol-gel method are potentially very exciting materials for applications in exotic fields like biotechnology and membrane reactors The material demands are high temperature stability narrow and uniform pore size distribution and high permeabilities Typical UF and RO membrane systems can be fabricated with these ceramic membrane modules In this area research can be extended to further narrow the pore sizes by deposition of inorganic species within the pores The present ultrafiltration membrane can then be used in the reverse osmosis role

2 Gas permeabilities of these ceramic membranes need to be tested For that, and proper selectivity of gaseous species much greater care need to be taken in membrane fabrication to prepare membranes with more uniform thickness which are completely free from microcracks

3 The experiments that have been carried out could be repeated in a stirred ultrafiltration cell using various other solutes like PVA Dextran and Black liquor to study membrane properties under steady state conditions

REFERENCES

1 H Lonsdale J Membrane Sc 10 (1982) 81

2 Munir Cheryan Ultrafiltration Handbook Technomic Publishing Co Inc Pennsylavania USA (1986)

3 E V Ballon and T Wijdeven J Colloid & Interface Sc 41 (1972) 198

4 J S Johnson Desalination 2 (1967) 243

5 I K Bansal AIChE Symp Ser 73 (1977) 144

6 B E Yoldas Am Ceram Soc Bull 54 (1975) 286

7 B E Yoldas J Mater Sc 10 (1975) 1856

8 B E Yoldas, Am Ceram Soc Bull 54 (1975) 289

9 Kaiser and Schmidt J Non Cryst Solids 63 (1984) 261

10 A F M Leenaars, K Keizer and A J Burggraaf, J Mater Sc 19 (1984) 1077

11 A F M Leenaars, K Keizer and A J Burggraaf J Colloid & Interface Sc , 105 [1] (1985) 27

12 A F M Leenaars, K Keizer and A J Burggraaf J Membrane Sc 24 (1985) 245

13 A F M Leenaars K Keizer and A J Burggraaf J Membrane Sc 24 (1985) 261

14 Membrane Handbook (Ed W S Winston Ho and Kamalesh K Sarkar Van Nostrand Reinhold New York (1992)

15 A J Burggraaf, H J M Bowmeester B A Boukamp R J R Uhlhorn and V Zaspalis in Science of Ceramic Interfaces (Ed J Nowotny) Elsevier Science Publishing Co Inc New York (1991) 525

28 W Van Praag V T Zaspalis K Keizer J G Van Ommen J R H Ross and A J Burggraaf EuroCeramics (Vol 3) Elsevier (Ed G de With R A Terpestra and R Metselar) 3 605

29 T Yamaki H Maeda K Kusakabe and S Morooka J Membrane Sc 85 (1993) 167

30 C J Brinker and G W Scherer Sol Gel Science Academic Press Inc (1990)

31 T Assih A Ayral M Abenoza and J Phalipou J Mater Sc 23 (1988) 3326

32 S M Wolfrum J Mater Sc Lett 6 (1987) 706

33 S J Wilson and M H Stacey J Colloid & Interface Sc 82 [2] (1981) 507

34 S J Wilson Mcconnell and M H Stacey J Mater Sc 15 (1980) 3081

35 Annual book of ASTM Standards Section 3 Metals Test Methods and Analytical Procedures Vol 0 3 01 Metals- Mechanical Testing Elevated and Low Temperature Tests 795 Designation E 855-84

36 Powder Surface area and Porosity 2nd Ed Lowell and Shields Chapman and Hall (1984) 94

37 S Bhattacharjee and P K Bhattacharya J Membrane Sc 72 (1992) 149

38 M W Chudacek and A J Fane J Membrane Sc 21 (1984) 145

39 J G Wijmans, R S Nakao and C A Smolders J Membrane Sc 20 (1984) 115

40 F E Daves B Bariou and S Poyen, J Membrane Sc 50 (1990) 177

ANNEXURE - I

THEORITICAL DETERMINATION OF POROSITY OF THE MEMBRANES

Let n be the number of pores / unit mass of porous membrane If the pores are cylindrical with radius r and length h then the total volume of pores / unit mass of membrane material is equal to

$$\frac{\pi d^2}{4} \times h \times n$$

Let the total porosity of the membrane be P It is related to the sintered density by the relation

$$1 - \frac{\text{sintered density}}{\text{theoritical density}} = P$$

If theoritical density is ρ then sintered density = ρ (1-P)

Therefore volume of pores / unit volume of membrane

$$P = \frac{\pi d^2}{4} \times h \times n \times \rho (1-P) \qquad (1)$$

Assuming that condensation takes place on the curved surface of the the pores

Total available specific surface area $S = n \pi d h$

whence $n h = \frac{S}{\pi d}$

Substituting the value in (1)

$$P = \frac{\pi d^2}{4} \rho (1-P) \frac{S}{\pi d}$$

$$\frac{P}{(1-P)} = \frac{S d \rho}{4000}$$ where S is in m^2/gm

d is in nm

& ρ is in gm/cm^3

Using the value ρ = 3 65 gm/cm^3 for γ - Al_2O_3 the porosities of the membranes were calculated

MSP-1994-M-SHA-CER

1 Manta ... ,£

2 Cocam ...